Nanoelectromagnetics: Circuit and Electromagnetic Properties of Carbon Nanotubes

*Chris Rutherglen and Peter Burke**

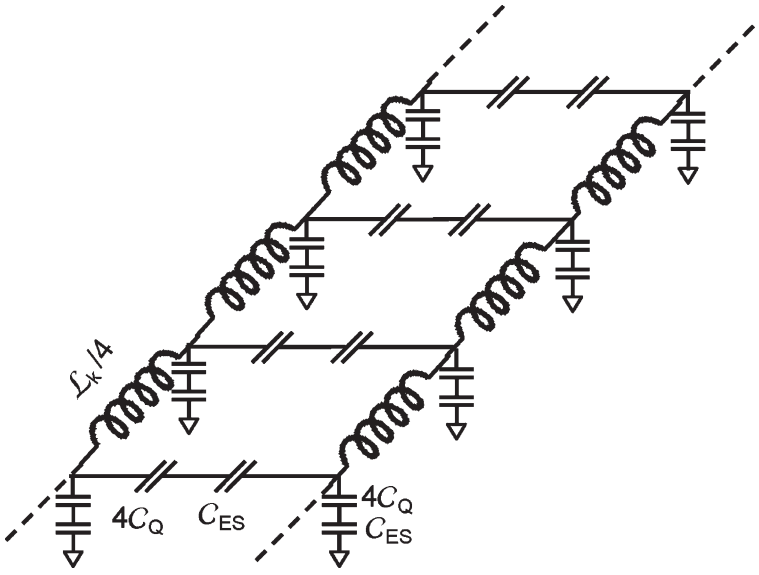

From the Contents

This Review presents a discussion of the electromagnetic properties of nanoscale electrical conductors, which are quantum mechanical one-dimensional systems. Of these, carbon nanotubes are the most technologically advanced example, and are discussed mainly in this paper. The properties of such systems as transmission electron microscopy waveguides for on-chip signal propagation and also the radiation properties of such systems are discussed. This work is primarily aimed at microwave, nanometer-wave, and THz electronics. However, the use of nanotubes as antennas in the IR and optical frequency range is not precluded on first principles and remains an open research area.

NANO MICRO small

1. Introduction

The development of fabrication and characterization techniques for nanoscale electronic circuit elements has been motivated by the relentless progress of the semiconductor industry in scaling down feature sizes. At the same time, clock rates of globally pervasive digital circuitry have moved into the microwave (GHz) frequency range. In addition, the growth in wireless communications systems has been explosive. The moniker ''anytime, anywhere'' access to information is no longer a goal but in many parts of the modern world is already here.

It seems then, that with the predicted progress towards nanometer-scale feature sizes, GHz clock rates, and microwave wireless communications as an ever increasing part of modern technology, that tremendous effort would already have been put into place to understand the properties of circuits, interconnects, devices, and antennas with nanoscale dimensions. Alas, such is apparently not the case. At present, there is a bona fide dearth of basic understanding of the electromagnetic properties of nanoscale conductors.

It is the aim of this paper to present some of the basic things we do know about nanoscale electromagnetics as examples of how circuit behavior is qualitatively different at nanometer-scale feature sizes. The focus is on *passive* devices. Active devices were reviewed in a separate recent manuscript.[1]

2. Scope and Aim of Review

The scope of this Review is as follows: The first goal is to present state-of-the art understanding of the ac properties of one-dimensional (1D) quantum conductors in the presence of damping (resistance). Here the 1D quantum nature of electron conduction gives rise to non-trivial circuit properties. One of the aims of this Review is to centralize, compare, and contrast different methods of analyzing the ac impedance of a quantum wire. The overarching theme is to answer a simple fundamental question, which is: What is the impedance of a quantum wire as a function of frequency from dc to light wave? This is a straightforward, scientific question to which a clear answer is beginning to emerge.

As part of the answer to this question we focus primarily on the RF and microwave frequency range of the spectrum, and thus use circuit models as the standard technique to present the electromagnetic properties. However, the formalism that justifies these circuit models can also be used to determine the optical equivalent properties such as scattering cross section.

In order to determine and illustrate the quantum ac properties of 1D systems, we focus on three important, canonical, illustrative cases: A single 1D wire over a perfect ground plane, a pair of 1D wires, and a pair of 1D wires over a perfect ground plane. In so doing, we also address and clarify the appropriate location of the quantum capacitance in the circuit diagram of a multi-1D conductor system.

Taken collectively this is meant to be a comprehensive review of the theoretical understanding of ac transport of 1D systems, and presented in a pedagogical and self-contained format. This is the prime aim of this Review.

A second aim is to assess the technological relevance of these models to the use of nanotubes as interconnects and antennas. Here we discuss the motivations for such comparisons and review the status of the field. The primary challenge here is the fabrication, and the word ''challenge'' here should be considered somewhat of an understatement. While there are still modeling results to be developed, there are some basic well-understood issues by now, which are the resistivity of nanotubes compared to copper, and the importance (or lack thereof) of the quantum properties of the conduction on the technology. Thus, while a comprehensive overview of the potential use of nanotubes as interconnects is not the goal of this Review, it is a major goal to relate the ac circuit models to the technological assessment of nanotubes as candidates for interconnects.

The conclusions of this paper will be that the 1D properties that give rise to non-trivial ac circuit models (specifically the kinetic inductance and quantum capacitance) are not really significant for technological concerns at GHz frequencies. For THz frequency electronics, which is still in its nascent stages, the quantum effects described in this work will be significant. The reason is simply that the resistance and classical electrostatic capacitance are more important in realistic potential applications. The resistance of a single tube is too high for envisioned applications (i.e., integration with Si CMOS) so that bundles are needed. The significance of the kinetic inductance and quantum capacitance in parallel arrays or bundles is even less than in individual 1D wires, so in this sense the quantum properties are not significant and are merely of academic interest. Of course, for the ultimate scaling of nanotechnology where each interconnect is a single-mode quantum wire, the theory results may be of significant importance but this is beyond what is envisioned in most proposed SWNT interconnect applications and would require some sort of self-assembly technology to even be considered as feasible. We have outlined such a vision in Reference [2] where single nanotubes interconnecting single-nanotube transistors are proposed.

A final aim of this Review is to summarize the state-of-the art experimental demonstrations illustrating some of the concepts presented theoretically. In this sense there are two major results, those of basic property measurements and actual interconnect fabrication and measurement. These are both reviewed and compared to the fundamental predicted performance limits discussed at the beginning of the paper.

2.1. Wavelength Versus Physical Dimension

For electromagnetic radiation with a wavelength of nanometers, one is in the X-ray range of the spectrum. Therefore, any technology with nanometer feature sizes is bound to be in the limit that the device size is much less than the wavelength.

[*] C. Rutherglen, Prof. P. Burke
Engineering Gateway 2232
Irvine, CA 92697–2625 (USA)
E-mail: pburke@uci.edu

DOI: 10.1002/smll.200800527

For RF engineering, this has been the case since its beginnings, since the wavelength is of the order of meters and the devices are many times smaller than this.

However, for optics, the concept of confining fields to subwavelength regions has been given recent interest, and the concept of an optical antenna has been proposed and demonstrated.[3,4] In addition, by making gratings subwavelength in size, and whispering gallery mode disks, subwavelength optics has taken on the moniker "'nano-optics". In some sense this is fundamentally new engineering and science. However, the concept of subwavelength physical sizes for diffraction gratings is almost as old as optics itself, and so is not truly new.

In the RF and microwave regime of the spectrum (the focus of this article), much less work has been done. It is generally the case the device sizes are subwavelength but this has never been touted as a fundamentally challenging issue to either understand or engineer. And, indeed, it is straightforward to understand and engineer.

2.2. DC Versus AC Eelectronic Properties

In the case of electronic properties of systems, there is another important wavelength, and that is the quantum-mechanical wavelength of the electron. At dc it is well known that when conductors are made at this scale the dc electronic properties are very different than larger conductors. Since the wavelength of electrons in metals and semiconductors is in the range 0.1–10 nm, this presents an important issue for dc properties of electronic devices. By and large, the physical principles that govern these device operations at dc have been fairly well laid out and understood by the device physics research community.[5] These concepts include, for example, the quantization of electrical conductance in units of $\frac{e^2}{h}$, and the concept of single-electron transistors, based on the large energy it takes to add a single electron to a system with a very small capacitance.

In contrast to dc, the physical principles that govern the ac (RF and microwave) electrical properties of electronic systems whose size scale is comparable to the quantum mechanical wavelength of electrons is not at all well understood. For example, a simple question is: What is the ac impedance of a 1D wire? Is it quantized in units of $\frac{e^2}{h}$ as the dc impedance is or not?[6] The answer to this question is not in general theoretically known, and to date experiments have not been performed that can unambiguously answer it.

2.3. Nanoantenna

A separate topic is the interaction of such systems with microwave radiation (e.g., plane waves). Until recently, very little was known about this at all. For example, if a nanotube is fabricated that is one free-space wavelength long, what will its radiation impedance be, what will the radiation pattern look like, how will the antenna resistive losses affect its properties, and what will the scattering properties be like? The answers to these questions are unknown for all but the very simplest of geometries, that of a dipole antenna geometry.[7,8] We do know from the dipole geometry studies that the properties are very different than textbook antenna theory predicts for a long, thin dipole. Thus, much remains to be understood.

P. J. Burke received his Ph.D. degree in physics from Yale University, New Haven, CT, in 1998, and was a postoc at Caltech until 2001. Since 2001, he has been with the Department of Electrical Engineering and Computer Science at the University of California, Irvine. He is the recipient of the ONR Young Investigator Award and the Army Research Office Young Investigator Program Award.

3. Carbon Nanotubes: Synthesis and Fabrication

Carbon nanotubes come in two varieties: single- and multi-walled.[9–15] In this paper we will be concerned primarily with single-walled carbon nanotubes (SWNTs), since they provide the simplest test cases for the concepts presented herein.

Since the original development of chemical vapor deposition (CVD) for nanotube synthesis from lithographically defined catalyst pads was developed in 1998,[13] many groups around the world have continued to focus on using CVD for synthesis. The basic concept of CVD is shown schematically in Figure 1. Many variations on this theme are possible, and progress in applying it to specific applications is rapid.

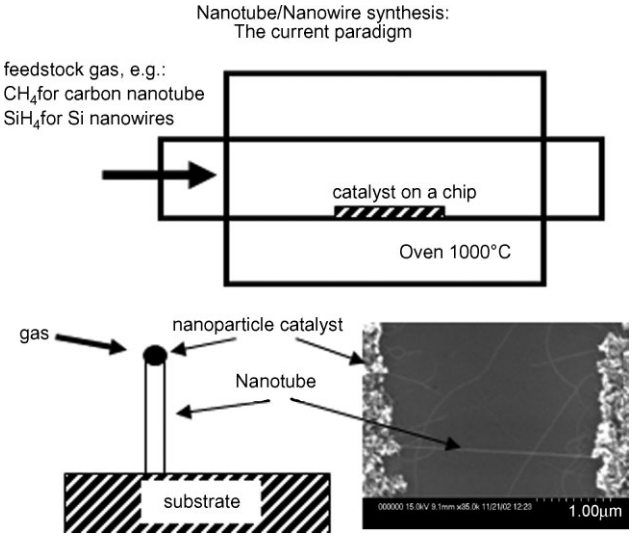

Figure 1. Typical synthesis paradigm, showing schematically how a carbon gas feedstock interacts with a catalytic nanoparticle to grow SWNTs.

small NANO MICRO

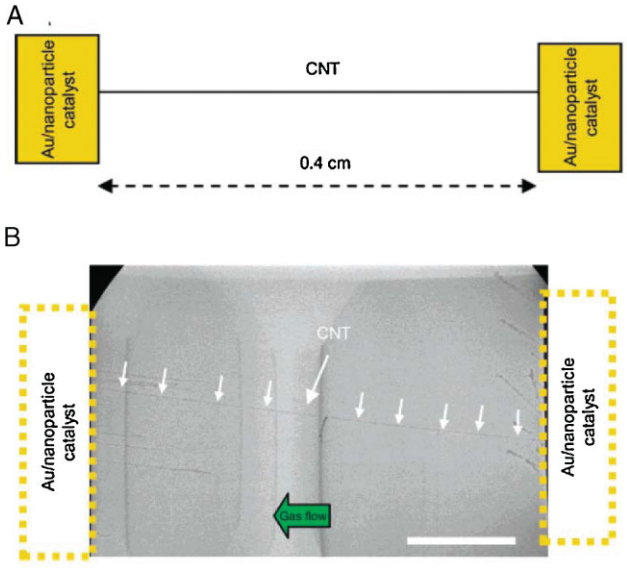

Figure 2. A) Schematic image of catalyst and CNT geometry. B) SEM image of individual CNT (sample A) bridging a 0.4-cm gap between two catalyst/electrode pads. Scale bar: 1 mm. Reproduced with permission from Reference [16]. Copyright 2004, Nano Letters.

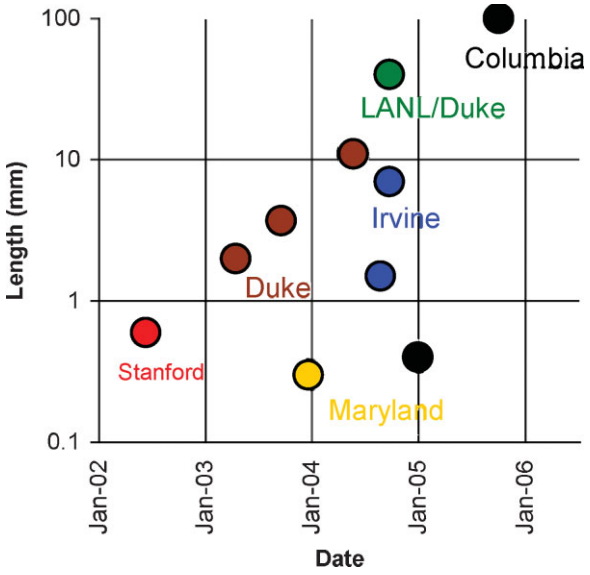

Figure 4. Length of individual SWNTs versus year (not necessarily electrically contacted), showing the rapid progress of nanotube synthesis technology over the past 10 years. Reproduced with permission from Reference [1]. Copyright 2007, World Scientific.

As an example of the rapid progress, in this section, we focus on a particular metric, that is, the synthesis of relatively long single-walled carbon nanotubes. The reason, as will become clear below, is that nanotubes may have a role to play as interconnects and the synthesis of long tubes is a necessary step in that direction. Additionally, long SWNTs allow one to measure the resistivity without worry about contact resistance effects. In Figure 2, we show an SEM image of an electrically contacted, 0.4-cm-long SWNT synthesized in our labs.[16]

In Figure 3, we show a plot of length versus year of electrically contacted, individual SWNTs. The progress has indeed been rapid. In addition, the tubes grown in CVD are highlighted in red, indicating that the growth technique has had a significant impact on the synthesis of long nanotubes. In Figure 4, we show the length versus year of all individual SWNTs. The progress has been about an order of magnitude increase in length per year. Such progress is rapid, even by the modern standards of electronics technology. It remains to be seen if and when such progress will plateau.

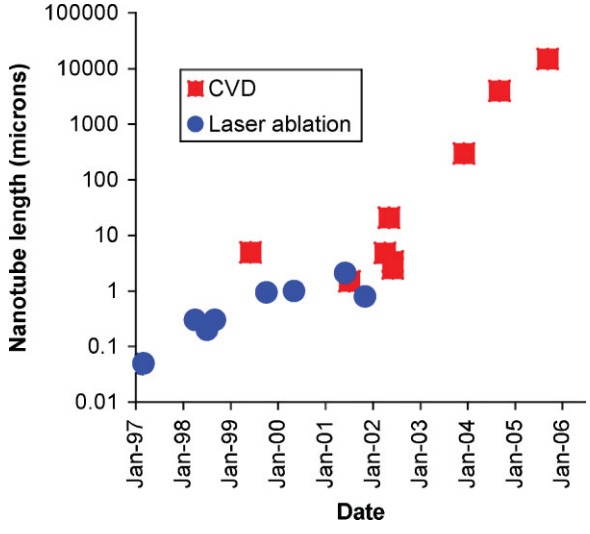

Figure 3. Length of electrically contacted individual SWNTs versus year, indicating the rapid progress of nanotube synthesis technology over the past 10 years. Reproduced with permission from Reference [1]. Copyright 2007, World Scientific.

4. Characterization

In this section we discuss some of the challenges associated with characterizing the electrical properties of nanoscale devices.

4.1. Quantum Versus Free-Space Impedance

In RF waveguides, the ratio of the RF voltage to the RF current is of order the characteristic impedance of free space, that is, 377Ω (see Figure 5). The ratio of the RF electric field to the RF magnetic field in free-space plane waves is also of order 377 Ω. (The same is true for optical plane waves, as well.) On the other hand, nano-electronic devices such as resistors with dimensions of order of the de Broglie wavelength of the electrons (typically the Fermi wavelength) have dc resistance values of order the resistance quantum $\frac{h}{e^2} = 25\,\mathrm{k}\Omega$.[5,17] The ratio of these two impedances is known as the fine structure constant α and is dependent on only three fundamental constants of the universe: the charge of the electron e, the speed of light c, and Planck's constant h. Therefore, there is an apparent built-in impedance mismatch between nanotechnology and RF. This mismatch has occupied the single-electron-transistor community for many years[18] and is now germane to the issue of nanotube-based devices.

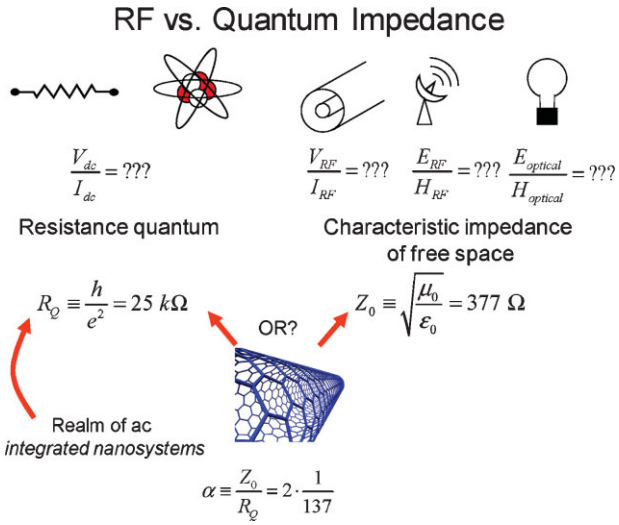

Figure 5. Quantum versus free-space impedance, indicating the inherent impedance mismatch between nanodevices (left) and free-space electromagnetic wave propagation (right). The purpose of this Review article is to address how a nanotube interacts with both of these physical realms. Reproduced with permission from Reference [1]. Copyright 2007, World Scientific.

4.2. Measurement Challenges

The above discussion shows that anytime the outside world is coupled at high frequency to a nanodevice, there is an inherent mismatch. This means that characterization, which is typically based on reflection, transmission, or scattering measurements, gives rise to very small signals: since the nanodevices are very small, they do not affect the microwaves very much. This is a big measurement challenge. One approach to solving this challenge is to develop excellent calibration techniques that fully characterize all of the parasitic before measuring the actual device. This is extremely time consuming, but certainly possible.[19–23] Another solution is to measure the change in the microwave properties with a dc voltage, which we have successfully applied in several cases.[24,25] However, one loses absolute accuracy with this technique. A final technique is to carry out measurements on many devices in parallel.[26–29] However, in general it is very difficult to fabricate identical nanodevices. Measurements on parallel devices can be plagued with uncertainties, since each individual device is different from the next.

Because of all of these challenges, the characterization requires serious effort by experimentalists in order to compare theory and models with experiment. In part because of this, theoretical work has been progressing relatively slowly.

5. DC Electronic Properties of Nanotubes

5.1. Metallic and Semiconducting Nanotubes

The electronic properties of SWNTs vary, depending on their diameter and chirality.[30] The chirality determines whether the nanotube behaves as a metal or semiconductor. Experimentally, metallic nanotubes are typically distinguished by the absence of a dependence of the small bias conductance on a gate voltage. Similarly, semiconducting nanotubes have a conductance that depends strongly on the gate voltage. The bandgap of semiconducting nanotubes is related to the diameter through $E_g = \frac{0.9eV}{d[nm]}$ where d is the diameter in nanometers.

5.2. Quantum Contact Resistance

A nanotube can be considered a 1D conductor, even at room temperature. It is by now well established that it is not possible to measure the resistivity of a 1D conductor using a four-terminal measurement: any terminal attached to the conductor destroys the 1D nature of the conduction.[5,31] Therefore, one can only perform a two-terminal measurement, and the contact resistance must be addressed.

For 1D systems that are in the ballistic limit (i.e., length less than the mean free path, mfp), the contact resistance is always greater than or equal to $\frac{h}{e^2} = 25\ k\Omega$. The difference between diffusive and ballistic transport is indicated schematically in Figure 6.

In SWNTs, this number is modified by a factor of 2 for band-structure degeneracy and a factor of 2 for spin,[30] so that the lowest possible resistance a SWNT can have (when it is shorter than the mfp) is $\frac{h}{4e^2} = 6\ k\Omega$. However, in cases where the contact is poor (e.g., if there is a Schottky barrier at the metal/nanotube interface), the resistance can be and typically is much higher. Recent work has shown that use of Pd as the contact material allows the theoretical limit to be reached, at least for very short SWNTs.[32–34] Prior to this, the more commonly used metal was Au and gave resistances of order MΩ, which was due to the poor contact.

5.3. Diffusive Resistance Versus Length

If the nanotube is long compared to the mean-free path due to scattering (l_{mfp}) then the resistance will have a component that scales linearly with length. In general, if R_c is

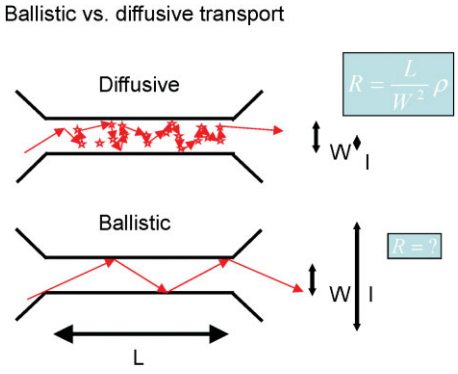

Figure 6. Ballistic versus diffusive transport, showing schematically a classical diffusive conductor (above), and a ballistic conductor with only contact resistance (below).

NANO MICRO small

the contact resistance (which is always greater than or equal to $\frac{h}{4e^2}$), then we have[31]

$$R_{dc} = R_c + \frac{h}{4e^2}\frac{L_{nt}}{l_{mfp}} \quad (1)$$

Exactly how long is the mean free path in a SWNT? This depends on the scattering rate and mechanism. As in other materials, it is common to classify the scattering as due to defects (which can vary depending on the quality of the nanotube), as well as phonons, which are present at finite temperature even for perfect (defect-free) material. An important practical question is, which mechanism dominates? In general the answer to this question depends on temperature and also (importantly) the way in which the nanotube material is synthesized and processed, since this determines the defect density. Overall, the working hypothesis is that the scattering rates add, that is,

$$\tau_{total}^{-1} = \tau_{e-ph}^{-1} + \tau_{imp}^{-1} \quad (2)$$

where τ_{e-ph}^{-1} is the electron–phonon scattering rate, τ_{imp}^{-1} is the impurity scattering rate, and τ_{total}^{-1} is the combined scattering rate. This would translate into a relationship between the electron–phonon mean free path l_{e-ph}, the impurity mean free path l_{imp}, and the combined mean free path l_{mfp}, of

$$\tau_{mfp}^{-1} = \tau_{e-ph}^{-1} + \tau_{imp}^{-1} \quad (3)$$

5.3.1. Impurity Scattering

The impurity mean free path depends in general on the density of impurities. Note that impurities outside the nanotube (such as in the substrate) can in principle cause scattering, as well as impurities in the nanotube itself. At the moment there are no good characterization techniques to determine impurity distribution on nanotubes, so in general it is not easy to know the impurity density. Collins' group has developed a technique using electroplating of nanotubes deposited on silicon wafers to image defects on nanotubes.[35] (Defect sites on nanotubes are found to be nucleation sites for electrodeposition of metals.) They find an impurity every 100 nm or so in arc discharge grown tubes, and every $\approx 0.4\,\mu m$ in CVD-grown nanotubes (depending on the CVD process), with some CVD nanotubes showing one defect per $\approx 100\,\mu m$. Therefore, a range of $\approx 100\,nm$ to $\approx 100\,\mu m$ for the impurity mean free path seems a reasonable range based on experimental data. Also, in general, the impurity mean free path is nominally independent of temperature, which provides an experimental means to distinguish it from electron–phonon scattering.

5.3.2. Electron–Phonon Scattering

Electron–phonon coupling in nanotubes is today well understood both from an experimental and theoretical point of view, and certainly very important for RF applications. For low voltages and currents, the scattering is due to acoustic phonons, whereas at high electric fields (discussed below), optical phonon scattering can be significant. The acoustic phonon scattering rate can be calculated based on the deformation potential,[36] and is predicted to be of the order of 1 μm, and also to depend on the nanotube diameter (scaling as the inverse diameter). The electron–phonon scattering rate is also predicted to be directly proportional to temperature. As we discuss next, the temperature dependence and magnitude of l_{e-ph} has been verified experimentally, while the diameter dependence is still untested, although generally believed to be true.

5.3.3. Length-Dependent Resistance in the Low-Bias Regime: Experimental Data

The dependence of resistance on length of a nanotube is an important issue for potential use as interconnects. Let us begin by assuming the nanotube is defect free (so that impurity scattering is negligible), and that the nanotube has perfect contacts (i.e., the contact resistance is $\frac{h}{4e^2}$). In that case, for nanotubes much shorter than the mean free path due to phonon scattering (i.e., much shorter than about 1 μm), the resistance will be equal to the contact resistance, and independent of the length. For nanotubes much longer than the phonon mean free path, the resistance will scale linearly with length, according to the following equation

$$R_{dc} \approx \frac{h}{4e^2}\frac{L_{nt}}{l_{mfp}} \quad (4)$$

(which is Equation (1) neglecting the contact resistance). Note that since the phonon mean free path is of order $\approx 1\,\mu m$ that the resistance per unit length is about $\frac{h}{e^2}$ per μm, or about $6\,k\Omega/\mu m$.

In general, if there is impurity scattering, the above discussion will still give the same predictions if the impurity scattering length is much longer than the electron–phonon mean free path. However, if there are many impurities, then the mean free path will be modified according to Equation (3).

The first experiments to probe the length-dependent resistance were performed by McEuen's group in 2004,[36] using an AFM to measure the potential drop along the length of the tube. These studies were for tubes up to 2 μm in length. In the same year, our group published the first resistance measurements on mm-long SWNTs,[16] and we compiled a plot of all the literature of resistance versus length (in both the short-tube and long-tube limit). Both our studies and McEuen's studies found that a mean free path of approximately 1 μm described the data to date. In 2007, the Kim group at Columbia published a landmark comprehensive study of the length- and temperature-dependent resistance of a single nanotube with multiple contacts, in order to rule out nanotube-to-nanotube variations.[37] We have compiled the results of all of these studies and plot in Figure 7 the room-temperature resistance versus length for single-walled nanotubes.[16,24,32,34,36–40] (Note that many early experiments on nanotubes used Au as the contacts and nanotubes less than 1 μm in length. In those early experiments, the contact resistance was much higher than the theoretical lower limit of $\frac{h}{4e^2}$ and so masked any length-dependent resistance.) The data

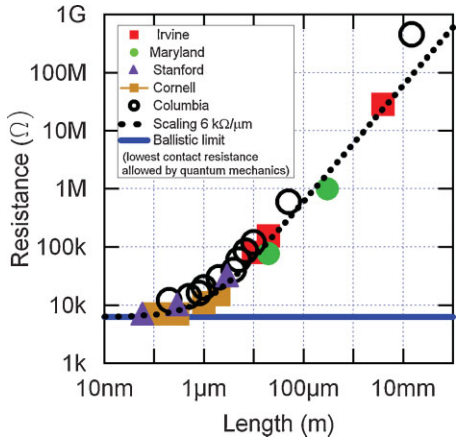

Figure 7. Room-temperature resistance versus length of individual SWNTs from various labs around the world. The Cornell data are on a single nanotube using an AFM to measure the voltage drop. The Columbia data are on a single nanotube with multiple contacts. The other data are for distinct nanotubes. The data collapse onto a single curve indicating a resistance per length of about $\frac{6\,k\Omega}{\mu m}$. Reproduced with permission from Reference [1]. Copyright 2007, World Scientific.

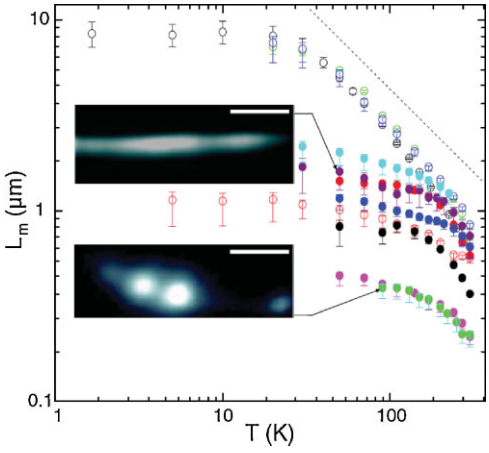

Figure 8. The electron mean free path versus temperature for the samples listed in Purewal at different temperatures.[37] Most metallic SWNTs (open circles) saturate at higher values than that of semiconductors (closed circles). The dashed line represents T^{-1} dependence. The insets show scanning gate microscopy images taken on two devices. Lighter color corresponds to less current in the SWNT. The defects in the SWNT are highlighted by the bright region (suppressed current) on the SWNT. The scale bar is 500 nm. Reproduced with permission from Reference [37]. Copyright 2007, Physical Review Letters.

are well described by Equation (1) above, using a mean free path of about 1 μm.

Is the scattering mechanism dominated by phonons or impurities? The theoretical prediction is that the phonon mean free path is approximately 1 μm, so the data indicate that phonon scattering dominates. The Kim group studied several different nanotubes (with different defect densities, presumably) and complied the measured mean free path versus temperature, which is reproduced in Figure 8. For the lowest defect density tubes, the mean free path at low temperatures can be as long as 10 μm. In this low-temperature limit, the impurity scattering dominates so that the mean free path is temperature independent. At room temperature, the mean free path depends approximately linearly on temperature, and is approximately 1 μm. This is clearly the phonon-scattering-dominated regime. For other nanotubes with more defects, the impurity scattering can be significant even at room temperature.

The combined conclusion of all of these studies is simple: for ideal (defect free) nanotubes, the room-temperature mean free path due to phonon scattering (which is unavoidable) is approximately 1 μm. This has been independently confirmed by multiple research groups around the world. The diameter dependence has not yet been established experimentally, but the mean free path is predicted to scale as the diameter linearly.

How does this theoretical limit compare to conventional metals? Remarkably, this indicates as 3D resistivity (assuming a diameter of 1.5 nm) of 1.1 μΩ cm, which is lower than bulk copper (which has a value of 1.7 μΩ cm). If a tightly packed array of SWNTs could be synthesized economically, the material would be a potentially disruptive technology for interconnects in integrated circuits. This motivates our discussion of the high-frequency properties of single-walled nanotubes as conductors.

5.4. High Bias Resistance

At high bias voltage, the current in metallic nanotube saturates. This was originally studied by Yao in 2000,[41] and is well established experimentally by now. The physical origin of the change in the high bias resistance is simple. If the electric field is strong enough, electrons in the nanotube gain energy as they accelerate. If they gain enough energy to be able to emit an optical phonon (which is typically only possible in high electric fields), then there is another scattering mechanism (optical phonon emission) which dramatically increases the scattering rate, and decreases the mean free path. Whereas the electron–phonon scattering rate for low electric fields and small currents is of order 1 μm due to acoustic phonon scattering, for high fields it is typically of order 10 nm due to optical phonon scattering. This scattering mechanism leads to a non-linear current–voltage curve that can be described by:

$$\frac{V}{I} = R_0 + \frac{V}{I_0} \tag{5}$$

where R_0 is the low bias resistance, and I_0 is given by $\frac{4e}{h}\hbar\Omega$, where $\hbar\Omega$ is the optical phonon energy. Typically I_0 is approximately 20 μA.

What is the importance of this high bias resistance on the potential use of nanotubes as interconnects? This issue concerned Roy, who proposed a step-wise model of the nanotube resistance for use in circuit simulators.[42–44] However, subsequent detailed analysis by the Meindl group showed that the high bias resistance is not of practical concern when nanotubes are used as interconnects.[45] In practical envisaged applications, the nanotubes would be long enough (and an array would be used), so that the electric field in the

NANO MICRO small

nanotubes would not be sufficient to cause the resistance to be much larger than its small bias value. For short nanotube interconnects, the driver resistance would be more important than the nanotube resistance. Thus, the conclusion of is that the high bias resistance can be neglected in practical applications.[45]

6. AC Electronic Properties of SWNTs

6.1. Motivation

At present, the propagation of high-frequency signals on high-performance modern integrated circuits is performed using copper interconnects. The bulk resistivity of copper is about 1.7 $\mu\Omega$ cm. However, as the copper feature size shrinks below 100nm,[46] surface scattering increases this resistivity.[47] On the other hand, as we discuss above, carbon nanotubes have lower resistivity than copper, as they are not negatively impacted by surface scattering. In addition, the current density achievable in carbon nanotubes ($\approx 10^9$ A cm^{-2}) is larger than that achievable in Cu ($\approx 10^7$ A cm^{-2}), due to electromigration problems. Synthesis and placement problems notwithstanding, these arguments provide strong motivation for investigating carbon nanotubes as interconnects in GHz integrated circuitry.

6.2. Background

The RF circuit properties of a 1D conductor were originally discussed by Wesstrom,[48] who developed a transmission line description. However, at the time the technology to experimentally address the concepts was lacking. In a related set of papers, theoretical physicists have been considering the ac impedance of 1D conductors from the Luttinger liquid point of view for over a decade.[49–56] We have recently applied the concepts of transmission line theory to develop a general RF circuit model for a single-walled nanotube.[57–60] Salahuddin has generalized this approach to include multimode quantum wires.[61] Such a circuit model consists of distributed electrostatic capacitance and magnetic inductance, just as a classical transmission line. However, the model also includes quantum capacitance and kinetic inductance, which are absent in a classical transmission line. These extra elements describe a transmission line with characteristic impedance of order the resistance quantum, and a wave velocity of order $c/100$. Thus, the use of nanotubes as interconnects can allow one to stay in the realm of the resistance quantum even for transmission line work, and avoid the problems of impedance matching of active devices to the characteristic impedance of free space.

6.3. Approaches to the Problem

There are many ways to solve problems in applied physics, such as the question of the electromagnetic properties of carbon nanotubes. The most general technique is to write Maxwell's equations and Schrödinger's equations, and claim that the problem is solved in principle. This is the most general technique, but not the most useful.

To date in the literature three separate techniques of solving the electromagnetics of carbon nanotubes has been put forth, some more general, and some more useful. The first approach is simply to write down the full 3D version of the Boltzman transport equation (BTE), and the boundary conditions on Maxwell's equations, and claim generality and completeness. This most general approach, which was developed by Slepyan and co-workers,[62–67] we shall call the ''Belarus method'' (even though many authors from other countries also contributed). The second method is to write down the one-dimensional versions of the Boltzman transport equation, and to develop equivalent circuit models based on this. This technique was developed recently by three authors at Purdue University (Salahuddin, Lundstrom, and Datta),[61] and hence we will call this the ''Purdue method''. It is more straightforward to apply to real-world problems, since it contains equivalent circuit descriptions of the physical phenomena. The third approach was developed by the current authors, and develops circuits from simple physical arguments.[57–60] While the least rigorous, it is perhaps the most applicable to real world situations, since it aims to understand currents and voltages at all points in a nanotube circuit. We call this third method the ''Irvine method''.

Below we discuss each of these techniques and compare their achievements to date, and their advantages and drawbacks. We also show that all three techniques give the same result in cases where there are overlapping predictions.

6.4. Are Quantum Correlations Important?

It should be noted that the role of quantum correlations between electrons, which historically has lead to dramatic unpredicted discoveries in condensed matter physics of 3D and 2D systems such as superconductivity and the quantum hall effect, are not completely understood in 1D systems in spite of great theoretical effort.[68] The arguments presented below are the state of the art in understanding electromagnetics of 1D systems, but not necessarily the final answer. In general, the practical effect of quantum correlations on nanotube devices and circuits is at present not known. At least one publication claims that the correlations will have an experimentally observable effect on this inductance per unit length of a 1D wire, which is not predicted in any of the more elementary theory discussed in this paper.[69]

Therefore, this paper should be viewed as a first effort to theoretically understand nano-electromagnetics without knowing for sure the effect of quantum correlations.

6.5. Voltage or Electrochemical Potential?

When dealing with most metals, the voltage is what matters. However, the electrochemical potential is what matters when dealing with systems that have a finite density of states (DOS). In nanotubes, the DOS is finite, and adding charge changes the Fermi energy, hence the chemical potential. The question is, which to use? For a SWNT over

a ground plane, Salahuddin et al. have shown that the electrochemical potential is what obeys a transmission line equation.[61] This will be discussed in more detail below.

6.6. High-Field Effects

It has been shown that high-electric-field effects limit the current in an individual SWNT to about 25 μA.[41] We have also observed this in microwave experiments on SWNTs at high electric fields.[25] The models developed below are all for the low-electric-field limit. More sophisticated models for the microwave properties at both high- and low-electric-field limits, which are technologically important for reasonable current and voltage levels in circuits, are still not well understood. Recent work has taken phenomenological approaches to very simple test cases,[45,70,71] but much work remains to be done to understand the high-field limit.

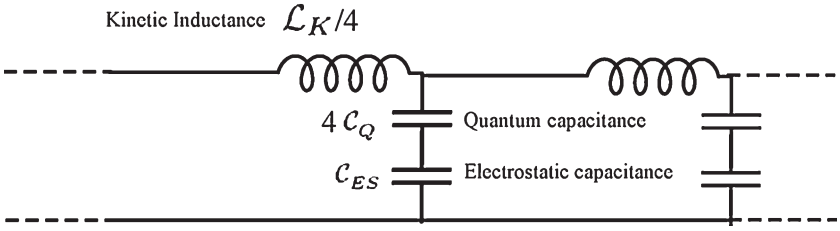

Figure 10. Single nanotube over ground plane circuit model. The three elements are the kinetic inductance, the quantum capacitance, and the electrostatic capacitance. All are distributed elements. The factor of 4 is for the band structure and spin degeneracy in SWNTs. Reproduced with permission from References [58, 60]. Copyright 2002, IEEE Transactions on Nanotechnology.

7. Individual Nanotubes Over Ground Plane: The Irvine Method

We begin our discussion by discussing the ac electrical properties of an individual metallic SWNT over a ground plane, indicated schematically in Figure 9. Figure 10 shows the equivalent RF circuit model for a SWNT over a highly conducting ground plane, neglecting damping.[58,60] In this approach, we derive independently each of the three circuit elements in the figure. The advantage of this approach is that one starts from the beginning with Kirchoff's laws of currents and voltages, and hence is immediately in the practical, experimentally accessible world. The disadvantage is the lack of rigor and generality, which we will discuss further as we continue.

7.1. Spin and Band-Structure Degeneracy

The dc circuit model for a one-channel quantum wire of non-interacting electrons is well known from the Landauer–Büttiker formalism of conduction in quantum systems. The dc conductance is simply given by e^2/h. If the spin degree of freedom is accounted for, there are two "channels" in a quantum wire: spin up and spin down, both in parallel. In a SWNT, there are two independent channels for each spin up electron, and two for each spin down electron, due to the band-structure degeneracy.[30] Thus, there are 4 independent channels. Since these channels are in parallel, the dc conductance is given by $4e^2/h$. In the discussions below, this factor of 4 (for the number of channels) will be important for nanotube RF circuit properties, also.

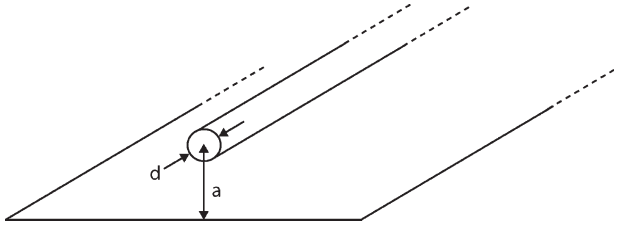

Figure 9. Geometry of a single nanotube over ground plane used to calculate the magnetic inductance and electrostatic capacitance. Reproduced with permission from References [58, 60]. Copyright 2002, IEEE Transactions on Nanotechnology.

7.2. Magnetic Inductance

In the presence of a ground plane, the magnetic inductance per unit length is given by:[72]

$$L_{\mathrm{M}} = \frac{\mu_{\mathrm{M}}}{2\pi}\cosh^{-1}\left(\frac{2a}{d}\right) \approx \frac{\mu_{\mathrm{M}}}{2\pi}\ln\left(\frac{a}{d}\right) \tag{6}$$

where d is the nanotube diameter, a is the distance to the "ground plane" (see Figure 9), and μ_{M} is the magnetic permeability of the medium. The approximation is good to within 1% for $a > 2d$. This is calculated using the standard technique of setting the inductive energy equal to the stored magnetic energy:

$$\frac{1}{2}L_{\mathrm{M}}I^2 = \frac{1}{2\mu_{\mathrm{M}}}\int B(x)^2 d^3x \tag{7}$$

and using the relationship between I and B in the geometry of interest, in this case a wire on top of a ground plane. For a typical experimental situation, the nanotube is on top of an insulating (typically oxide) substrate, with a conducting medium below. (The finite conductivity of the conducting medium will be discussed below.) A typical oxide thickness is between 100Å and 1 μm, whereas a typical nanotube radius is 1nm. Because the numerical value of L_M is only logarithmically sensitive to the ratio of d/h, we can estimate it within a factor of three as:

$$L_{\mathrm{M}} \approx 1^{pH}/\mu\mathrm{M} \tag{8}$$

We use μm for our length units because modern growth processes produce nanotubes with lengths of order micrometers and not (as of yet) meters.

NANO MICRO small

7.3. Kinetic Inductance

In order to calculate the kinetic inductance per unit length, we calculate the kinetic energy per unit length and equate that with the $\frac{1}{2}L_M I^2$ energy of the kinetic inductance. The kinetic energy per unit length in a 1D wire is the sum of the kinetic energies of the left-movers and right-movers. If there is a net current in the wire, then there are more left-movers than right-movers, say. This argument is indicated schematically in Figure 11.

If the Fermi level of the left-movers is raised by $e\Delta\mu/2$, and the Fermi level of the right-movers is decreased by the same amount, then the current in the 1D wire is $I = \frac{e^2}{h}\Delta\mu$. The net increase in energy of the system is the excess number of electrons ($N = e\Delta\mu/2\delta E$) in the left versus right moving states times the energy added per electron $e\Delta\mu/2$.

Here δE is the single-particle energy-level spacing. In a 1D system of length L_{nt}, the spacing between quantum states is given by:

$$\delta E = \frac{dE}{dk}\delta k = \hbar v_F \frac{2\pi}{L_{nt}} \tag{9}$$

where we have assumed a linear dispersion curve appropriate for carbon nanotubes. Thus the excess kinetic energy is given by $hI^2/4v_F e^2$. By equating this energy with the $\frac{1}{2}L_K I^2$ energy, we have the following expression for the kinetic energy per unit length:

$$\mathcal{L}_K = \frac{h}{2e^2 v_F} \tag{10}$$

This is the kinetic inductance per unit length for a single channel. Since a nanotube has 4 channels in parallel, the effective circuit diagram in Figure 10 includes a factor of $\frac{1}{4}$ for the (total) kinetic inductance. The Fermi velocity for graphene and also carbon nanotubes is usually taken as $v_F = 8 \times 10^5$ ms^{-1}, so that numerically

$$\mathcal{L}_K = \frac{4nH}{\mu m} \tag{11}$$

Note that just because the total energy of the system scales as the current squared ($E \propto I^2$), that does not necessarily prove that the circuit properties will be inductive. Thus the rigor of this approach is not total. On the other hand the intuition about the origin of the kinetic inductance is very clear in the context of the Landauer–Büttiker formalism of conduction.

It is interesting to compare the magnitude of the kinetic inductance to the magnetic inductance. From Equations (6) and (10), we have

$$\frac{\mathcal{L}_M}{\mathcal{L}_K} = \alpha \frac{2}{\pi}\frac{v_F}{c}\ln\left(\frac{a}{d}\right) \sim 10^{-4} \tag{12}$$

where $\alpha \approx 1/137$ is the fine structure constant.

Thus, in 1D systems, the kinetic inductance will always dominate. This is an important point for engineering nanoelectronics: In engineering macroscopic circuits, long thin wires are usually considered to have relatively large (magnetic) inductances. In the case of nanowires, the magnetic inductance is not that important; it is the kinetic inductance that dominates.

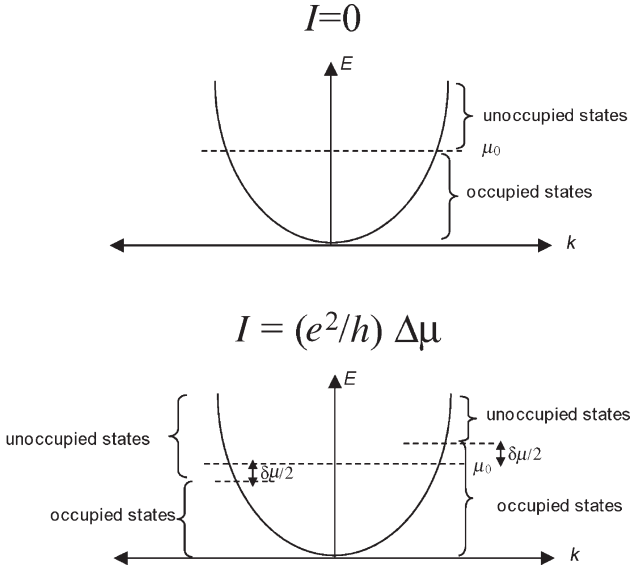

Figure 11. Dispersion curve for zero and non-zero current in a 1D conductor. The quantum states below the dotted line are occupied, and those above the dotted line are empty. When there are more right-going than left-going quantum states occupied (bottom), there is a net current. The excess energy scales as the current squared, which can be used to calculate the kinetic inductance.

7.4. Electrostatic capacitance

It is generally believed that the effect of electron-electron interactions can be included in the transmission line circuit analogy as an electrostatic capacitance.[68]

The electrostatic capacitance between a wire and a ground plane as shown in Figure 9 is given by:[72]

$$C_{ES} = \frac{2\pi\varepsilon_D}{\cosh^{-1}(2a/d)} \approx \frac{2\pi\varepsilon_D}{\ln(a/d)} \tag{13}$$

where again the approximation is good to within 1% for $h > 2d$.

This can be approximated numerically as

$$C_{ES} \approx 50aF/\mu m \tag{14}$$

This is calculated using the standard technique of setting the capacitive energy equal to the stored electrostatic energy:

$$\frac{Q^2}{2C_{ES}} = \frac{\varepsilon_D}{2}\int E(x)^2 d^3x \tag{15}$$

and using the relationship between E and Q in the geometry of interest, in this case a wire on top of a ground plane. The term ''electrostatic'' comes from the approximation that we make in calculating the capacitance using Equation (15), which is done

using the relationship between a static charge and a static electric field. However, the electrostatic capacitance can of course be used when considering time-varying fields, voltages, currents, and charges, as we will do below.

7.5. Quantum Capacitance

In a classical electron gas (in a box in 1, 2, or 3 dimensions), to add an extra electron costs no energy. (One can add the electron with any arbitrary energy to the system.) In a quantum electron gas (in a box in 1, 2, or 3 dimensions), due to the Pauli exclusion principle it is not possible to add an electron with energy less than the Fermi energy E_F. One must add an electron at an available quantum state above E_F. This is indicated schematically in Figure 12.

By equating the energy cost to add an electron δE (see Equation (9)) with an effective quantum capacitance with energy given by

$$\frac{e^2}{C_Q} = \delta E \tag{16}$$

and considering the degeneracy, one arrives at the following expression for the (quantum) capacitance per unit length:

$$C_Q = \frac{8e^2}{h\upsilon_F} \tag{17}$$

which comes out to be numerically

$$C_Q = 400\,aF/\mu m \tag{18}$$

This is the quantum capacitance per unit length for a single channel. Since a nanotube has 4 channels in parallel, the effective circuit diagram in Figure 10 includes a factor of 4 for the (total) quantum capacitance. The ratio of the electrostatic to the quantum capacitance is then given by

$$\frac{C_{ES}}{C_Q} = \frac{2\pi a}{e^2\mu\upsilon_F}\ln\left(\frac{a}{d}\right) = \frac{1}{\alpha}\frac{2}{\pi}\frac{\upsilon_F}{c}\ln\left(\frac{a}{d}\right) \sim 1 \tag{19}$$

Thus, when considering the capacitive behavior of nanoelectronic circuit elements, both the quantum capacitance and the electrostatic capacitance must be considered.

In addition, it should be noted that within the context of this argument, it is not proved why the fact that the energy of the system increases when the charge increases that this should behave as a capacitor when inserted into a circuit. Again, this is where the rigor of this model fails. However, again, the physical origin of the quantum capacitance is quite clear in the context of the quantum properties of non-interacting electrons.

7.6. Resistance and Damping

From the above section, we have a reasonable estimate of the dc resistance per unit length of about $\frac{6k\Omega}{\mu m}$. Thus, if the ac damping is the same as the dc damping, the equivalent circuit model should include a resistance per unit length as well. The implications of this will be discussed in more depth below, where comparisons to copper are made.

8. Individual Nanotubes Over Ground Plane: The Purdue Method

The approach of the Purdue method, developed in,[61] is to begin with the one-dimensional Boltzman transport equation and then to derive from this the analog of the telegrapher equations relating the current $I(x,t)$ and electrochemical potential $\mu(x,t)$. From these telegrapher equations, one can infer the equivalent capacitance per unit length, and the inductance per unit length. As such the technique is more rigorous, although it provides a somewhat less clear description of the physical origin of the kinetic inductance. In his overview, we assume only one sub-band is occupied.

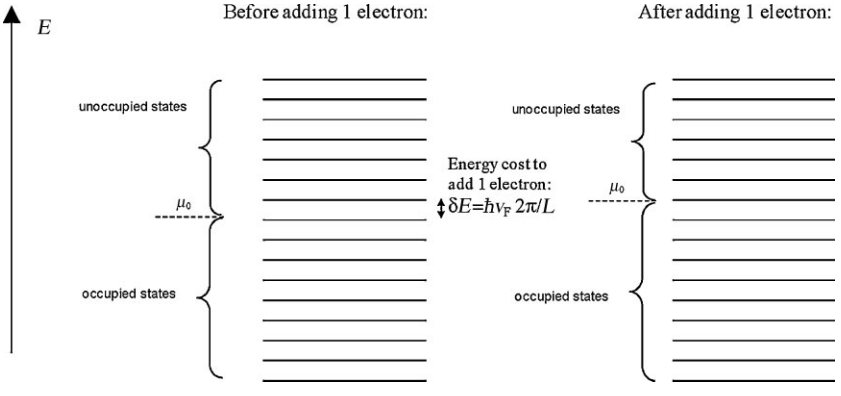

Figure 12. Quantum capacitance calculation. The discrete quantum energy levels for a particle in a (1D) box are shown. The states above the dotted line are empty, and the states below the dotted line are full. Adding an additional electron to the system costs ΔE of energy due to the finite spacing between the states. Thus, charging the system raises its energy, which is the concept of quantum capacitance, since in a classical system the energy spectrum is continuous and charging the system costs no energy.

8.1. Overview of Approach

In this approach, one starts with the 1D Boltzman transport equation:

$$\frac{\partial f}{\partial t} + \upsilon_x\frac{\partial f}{\partial x} - \frac{e}{\hbar}E_x\frac{\partial f}{\partial k} = S_{OP}f. \tag{20}$$

(In this paper, we take x as the long axis of the SWNT.) Here $f(x,k,t)$ is the probability that an electron will occupy position x at time t with wavevector k. At equilibrium, this is given by $f_0 = (1 + e^{E(x,k,t)/k_BT})^{-1}$. Here the interpretation of E is $E = \varepsilon(k) - \mu$, where ε(k) is

NANO MICRO small

the dispersion curve, and μ the chemical potential. S_{OP} is a forcing function describing the rate at which the system returns to equilibrium. Under an electric-field drive or other non-equilibrium situation, it is typical to assume local equilibrium so that the concept of a local chemical potential applies. In this case, the interpretation of E is $E = \varepsilon(k) + U(x,t) - \mu(x,t)$, where U is the electrostatic energy.

By multiplying the 1D BTE by υ and summing over k, one can derive the first of the telegrapher equations relating the time derivative of the current to the spatial derivative of the electrochemical potential:

$$\frac{\partial I}{\partial t} + \frac{I}{\tau} = -\frac{1}{L_K}\frac{\partial(-\mu/e)}{\partial x} \tag{21}$$

where

$$\frac{1}{L_K} \equiv \frac{e^2}{L_{nt}}\sum_k \upsilon^2\left(-\frac{\partial f_0}{\partial E}\right), \tag{22}$$

and where the phenomenological scattering time τ is defined in the usual way. Next, one derives the second of the telegrapher equations relating the time derivative of the electrostatic potential so the spatial derivative of the current in the usual way:

$$C_{ES}\frac{\partial V}{\partial t} = -\frac{\partial I}{\partial x} \tag{23}$$

If the chemical potential and electrostatic potential were equal (as is the case in metals with large DOS), one could approximate μ by U and then combine Equations (21) and (23) to come up with the wave equation. However, in 1D systems with a finite DOS, they are not equal. One can derive a relationship between μ and U using energy considerations, and find:[61]

$$C_{ES}\delta U = \frac{C_{ES}C_Q}{C_{ES}+C_Q}\delta\mu \tag{24}$$

This allows one to derive the wave equation as:

$$\frac{\partial^2 I}{\partial t^2} = \frac{1}{L_K C}\frac{\partial^2 I}{\partial x^2} \tag{25}$$

and

$$\frac{\partial^2 \mu}{\partial t^2} = \frac{1}{L_K C}\frac{\partial^2 \mu}{\partial x^2} \tag{26}$$

where C is C_Q in parallel with C_{ES}.

Note the electrostatic and quantum capacitance add inversely, as in the circuit diagram proposed using the Irvine method. Thus, this technique rigorously justifies the circuit diagram shown in Figure 10, provided one interprets it as a waveguide for the electrochemical potential.

8.2. Quantum Capacitance

In the Purdue method, the quantum capacitance is clearly defined as $d\rho/d\mu$,[61] which can related to the density of states through:

$$C_Q = \frac{e^2}{L}\sum_k\left(-\frac{\partial f_0}{\partial E}\right) \tag{27}$$

Thus, for 1D metallic nanotubes, C_Q given by the Irvine method is consistent with this.

8.3. Kinetic Inductance

The kinetic inductance given by Equation (22) is less clear than the Irvine method. If the dispersion curve is linear as for metallic nanotubes, it is shown in the kinetic inductance calculated the Irvine method is the same.[61]

9. Individual Nanotubes Over a Ground Plane: The Belarus Method

The Belarus method begins with the full 3D version of the BTE. In addition, this approach treats the nanotube as a tube of conducting 2D material. Finally, the Belarus method carefully considers the boundary conditions of the electromagnetic fields at the surface of the nanotube, which is very useful for radiation problems, to be discussed in the following sections. However, no mention of the quantum capacitance is provided and so in this sense the theory cannot yet provide circuit level information. Nonetheless we show in this section that the Belarus method does predict the kinetic inductance as both of the previous ways.

9.1. Outline of the Belarus Method

This discussions follows Slepyan.[65] One starts with the full 3d BTE:

$$\frac{\partial f}{\partial t} + \upsilon_x\frac{\partial f}{\partial x} - \frac{e}{\hbar}E_x\frac{\partial f}{\partial k_x} = S_{OP}[f] \tag{28}$$

Then, one relates the current to the velocity of each electron in the x direction (along the axis of the nanotube) using:

$$J_x = \frac{2e}{(2\pi\hbar)^2}\int\int \upsilon_x f d^2\mathbf{p} \tag{29}$$

where the integration is over the first Brillouin zone. Then one defines a conductivity of the 2d layer using:

$$J_x = \sigma_x(\omega,h)E_x \tag{30}$$

where

$$\sigma_{xx}(\omega,h) = i\frac{2e^2}{(2\pi\hbar)^2}\iint\frac{\partial F}{\partial p_x}\frac{\upsilon_x d^2\mathbf{p}}{\omega - h\upsilon_x + i\tau^{-1}}, \quad (31)$$

Note that this is the *sheet* conductivity of the walls of the nanotube, with units of Siemens. While Equation (31) above is fully general, it can be evaluated further if one knows the dispersion curve of the electrons. This is known for carbon nanotubes, and is evaluated for metallic (armchair) nanotubes to give:

$$\sigma_{xx} \approx -i\frac{4e^2\upsilon_F}{\pi h\, R(\omega + i\upsilon)}, \quad (32)$$

where R is the radius of the nanotube.

9.2. Kinetic Inductance

We now provide a continuation of Equation (32). If an electrode is attached to a nanotube, practically this means injecting current which is presumably uniformly distributed throughout the circumference of the nanotube. This means that the current will be related to the current density through $I = J2\pi R$. In addition, the voltage is related to the electric field through $E_x = \frac{V}{L_{nt}}$. So Equations (30) and (32) can be recast in the form:

$$V = E_x L_{nt} = \frac{J}{\sigma_{xx}}L_{nt} = \frac{I}{2\pi R}\frac{1}{\sigma_{xx}}L_{nt}$$
$$= \frac{1}{4}\frac{h}{2e^2\upsilon_F\tau}(1 + i\omega\tau)L_{nt} \quad (33)$$

where $\tau \equiv \frac{1}{\upsilon}$. The term linear in frequency behaves electrically as an inductance, hence it shows behavior given by:

$$L_K = \frac{1}{4}\frac{h}{2e^2\upsilon_F}L_{nt} \quad (34)$$

This is equivalent to the inductance derived using both approaches above, for example, Equation (10).

9.3. Quantum Capacitance

No mention of the quantum capacitance is given the Belarus method. This is because the neglect of the third term in the BTE in the derivation of Equation (32) above.

9.4. Electrostatic Capacitance

Because the Belarus method derives mainly scattering properties, the capacitance is not dealt with from a circuit point of view. However, in principle it could be incorporated.

10. Comparison of the Three Methods

All three methods yield identical answers when their areas of prediction overlap. In the following section, we extend the Purdue method to more complicated geometries, which is important for understanding crosstalk in nanotube and between nanotube interconnects.

11. Two-Nanotube Transmission Line

The approach we will take to this problem is the Purdue method. We will consider carefully the electrochemical potential and electrostatic potential of a two-nanotube transmission line. The Irvine method does not suffice to clarify the role of the quantum capacitance in the two-nanotube transmission line case. The geometry to be considered is shown in Figure 13 below. The equivalent circuit diagram, which will be justified in detail below, is shown in Figure 14.

11.1. Electrostatics

Consider a system of N conductors, each maintained at a specific potential. The energy of such a system is given by:

$$U = \frac{1}{2}\sum_i\sum_j C_{ij}Q_iQ_j \quad (35)$$

where C_{ij} is the capacitance matrix describing the conductors, and Q_i and Q_j are the charges on conductors i and j, respectively. The charges and potentials are generally related by:

$$Q_i = \sum_j C_{ij}V_j \quad (36)$$

In this section, we are interested in a symmetric geometry, so that it can be assumed that $C_{11} = C_{22}$, and $C_{12} = C_{21}$.

Now, let us write explicitly the equations for the case of 2 conductors:

$$Q_1 = C_{11}V_1 + C_{12}V_2 \quad (37)$$

$$Q_2 = C_{21}V_1 + C_{22}V_2 \quad (38)$$

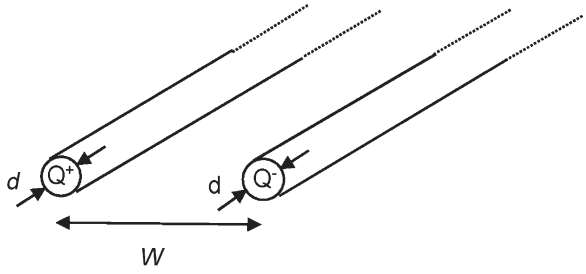

$$E = \frac{Q^2}{2C_Q} + \frac{Q^2}{2C_Q} + \frac{Q^2}{2C_{ES}}$$

Figure 13. Geometry of two parallel nanotubes used to calculate the magnetic inductance and electrostatic capacitance. Reproduced with permission from Reference [8]. Copyright 2002, IEEE Transactions on Antennas and Propagation.

NANO MICRO small

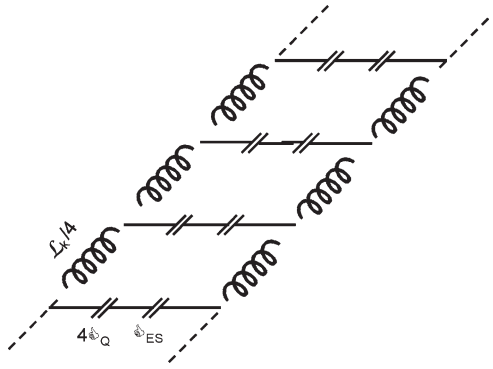

Figure 14. Circuit model for two-parallel-nanotubes model. The three elements are the kinetic inductance, the quantum capacitance, and the electrostatic capacitance. All are distributed elements. The factor of 4 is for the band structure and spin degeneracy in SWNTs. Reproduced with permission from Reference [8]. Copyright 2002, IEEE Transactions on Antennas and Propagation.

We are interested in the differential mode for this section, so let us define two variables:

$$\Delta Q \equiv Q_2 - Q_1 \tag{39}$$

$$Q_T \equiv Q_2 + Q_1 \tag{40}$$

and similarly

$$\Delta V \equiv V_2 - V_1 \tag{41}$$

$$V_T \equiv V_2 + V_1 \tag{42}$$

In this case, it can be shown that for the differential mode:

$$\Delta Q = \Delta V(C_{11} - C_{12}) \tag{43}$$

Thus, we have the electrostatic capacitance between the two tubes as:

$$C_{\mathrm{ES}(2)} = C_{11} - C_{12} \tag{44}$$

This will be useful later. Note that in terms of the geometry of two wires, this is given by:

$$C_{\mathrm{ES}(2)} \equiv \frac{\pi\varepsilon}{\cosh^{-1}\left(\frac{W}{d}\right)} \tag{45}$$

where the diameter is d, and the separation is W.

11.2. Quantum Capacitance

We seek to understand the quantum capacitance as it relates to the two-nanotube transmission line. This requires some thought. We will follow the approach used by Purdue. Refer to Figure 15.

In the top two figures, we have the dispersion curve for each wire, when no excess charge is found on either wire. In this case wire 1 has a chemical potential μ_{10}, and wire 2 has a chemical potential μ_{20}. Next, we consider the case where wire 1 has charge Q_1, and wire 2 has charge Q_2. First consider wire 1. By the definition of the quantum capacitance, the chemical potential of wire 1 changes according to:

$$\delta\mu_1 = \frac{C_Q \Delta Q_1}{e} \tag{46}$$

Here the small delta δ means a response to the charge on the tube. Similarly for wire 2, we have:

$$\delta\mu_2 = \frac{C_Q \Delta Q_2}{e} \tag{47}$$

Next, consider the relationship between the change in electron density δn_1 on wire 1 to the change in the electrostatic and chemical potential. The electrostatic energy changes by δU_1 due to the extra charge. Since the total energy E is written as:

$$E = \varepsilon_{\mathrm{m}}(k) + U - \mu(x,t) \tag{48}$$

we have

$$\delta n_1 = \frac{\partial n}{\partial E}(\partial U_1 - \partial\mu_1) \tag{49}$$

Thus

$$\begin{aligned} e^2\delta n_1 &= -e^2\tfrac{\delta n}{\delta E}(\delta\mu_1 - \delta U_1) \\ &= C_{11}\delta U_1 + C_{12}\delta U_2 \end{aligned} \tag{50}$$

where the last equality introduces the coupling between wires 1 and 2.
Similarly for wire 2:

$$\begin{aligned} e^2\delta n_2 &= -e^2\tfrac{\delta n}{\delta E}(\delta\mu_2 - \delta U_2) \\ &= C_{21}\delta U_1 + C_{22}\delta U_2 \end{aligned} \tag{51}$$

However, from Equation (27) we notice the definition of C_{Q}, so that we may rewrite these equations as:

$$C_{\mathrm{Q}}(\delta\mu_1 - \delta U_1) = C_{11}\delta U_1 + C_{12}\delta U_2 \tag{52}$$

$$C_{\mathrm{Q}}(\delta\mu_2 - \delta U_2) = C_{21}\delta U_2 + C_{22}\delta U_2 \tag{53}$$

We seek now a relationship between the difference in chemical potentials and the difference between electrostatic potentials, as:

$$\Delta U \equiv \delta U_2 - \delta U_1 \tag{54}$$

$$\Delta\mu \equiv \delta\mu_2 - \delta\mu_1 \tag{55}$$

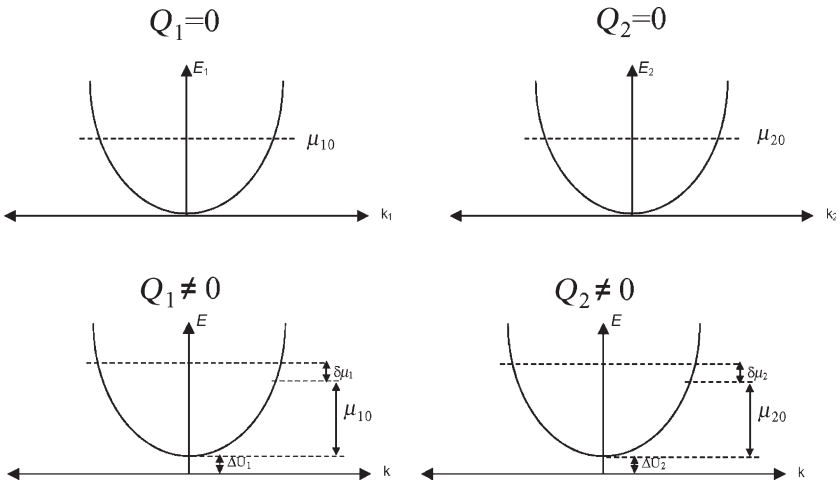

Figure 15. Two nanotube dispersion curves used to determine the quantum capacitance and electrostatic capacitance for two parallel nanotubes. Because the electrostatic capacitance deals with differential charge, whereas the quantum capacitance for each tube deals with charge per tube, the roles of both in a coupled system must be considered carefully.

which we can find from the above equations. We find:

$$(C_{11}-C_{12})\Delta U=\left(\frac{(C_{11}-C_{12})C_{\mathrm{Q}}}{(C_{11}-C_{12})+C_{\mathrm{Q}}}\right)\Delta\mu \tag{56}$$

Thus, the capacitance per unit length for this differential mode is given by (using the above $C_{ES}\equiv C_{11}-C_{12}$),

$$C\equiv\frac{C_{ES}C_{Q}}{C_{ES}+C_{Q}} \tag{57}$$

This justifies the capacitance in the circuit diagram of Figure 14. Note that the quantum capacitance has no factor of 2. We have included in Figure 14 the correct factor of 4 for band structure and spin degeneracy. Numerically, because of these factors of 4, after all this work, one finds the quantum capacitance is typically modifying the circuit by about 20%.

12. Two Nanotubes Over Ground Plane

In this section we consider the effective circuit model for two nanotubes over a ground plane. In Figure 16, we indicated the geometry schematically. In Figure 17, we indicate the appropriate circuit diagram.

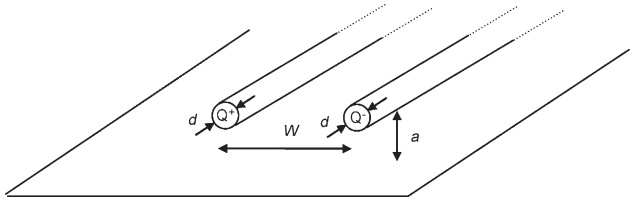

Figure 16. Geometry of two nanotubes over ground plane used to calculate the electrostatic capacitance and magnetic inductance.

The approach to justifying this circuit diagram is similar to that for the previous case, and will only be outlined here. In the case of a ground plane, there is a third conductor. However, we approximate it as an infinite capacitor with zero voltage at all times, regardless of the charge on the third conductor. The above analysis for the two-nanotube transmission line can still be applied. The new calculation that needs to be done is to determine the common mode chemical potentials and voltages. After such an analysis, one comes to the conclusion that the circuit diagram of Figure 17 is appropriate.

This circuit diagram is of practical importance as a basis for understanding crosstalk and (possibly) ground-bounce effects if nanotubes are to be used as interconnects in integrated circuits.

13. Interconnects

13.1. Comparison to Copper

The use of nanotubes as interconnects is motivated primarily by the low resistivity compared to copper.[73] The term ''resistivity'' is usually used for metals, and for nanotubes needs to be clearly defined. Here by nanotube resistivity, we use the same definition as for metals. For a single nanotube, the resistivity is lower than bulk copper. However, bulk copper resistivity values are not always attainable, due to enhanced surface scattering. So for narrow-line-width interconnects, the resistivity of Cu is larger than its bulk value. These principles are illustrated in Figure 18. For the copper resistivity, we have used the Fuchs/Sondheimer and Mayadas/Shatzkes model (Equations 4 and 5 in Steinhogl),[47] with the parameters $R=0.27$, $p=0.5$, $\lambda=45$ nm. For the SWNT, we use data from

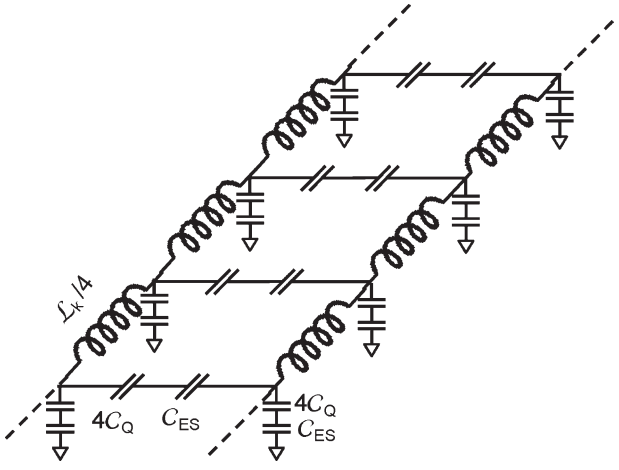

Figure 17. Circuit model for two nanotubes over a ground plane. The three elements are the kinetic inductance, the quantum capacitance, and the electrostatic capacitance. All are distributed elements. The factor of 4 is for the band structure and spin degeneracy in SWNTs.

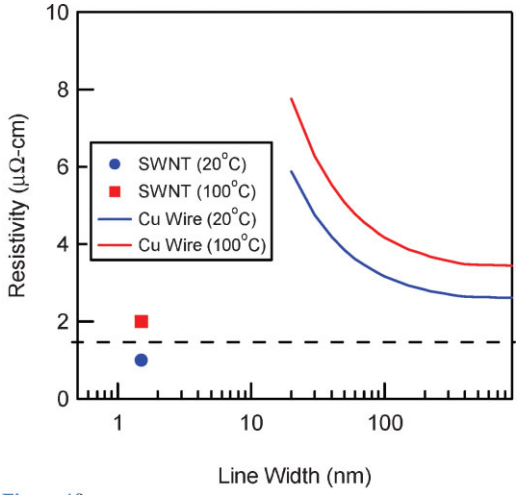

Figure 18. Resistivity versus diameter for copper and SWNTs at 20 °C and 100 °C. For the copper resitivity, we have used the Fuchs/Sondheimer and Mayadas/Shatzkes model (Equations (4) and (5) in Reference [47]) with the parameters R = 027, $p = 0.5$, $\lambda = 45$ nm. The dashed line is the bulk value for Cu. For the SWNT, we use data from Purewal, [37] extrapolating to ≈100 °C.

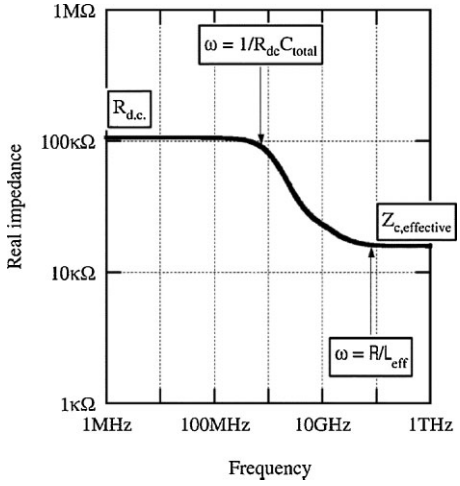

Figure 19. Simulated real impedance for a 100-μm-long SWNT, assuming a resistance per unit length of $\frac{1\,k\Omega}{\mu m}$. At dc the real impedance is simply the resistance per length times the length. As the frequency is increased, the impedance falls. The frequency scale at which the impedance starts to change is given by the inverse of the total capacitance times the total resistance. At very high frequencies, the impedance becomes equal to the effective characteristic impedance. The frequency at which this occurs is given by the inverse of the effective $\frac{L}{R}$ time constant, which is the resistance per unit length divided by the inductance per unit length. Reproduced with permission from Reference [57]. Copyright 2002, IEEE Transactions on Nanotechnology.

Purewal,[37] extrapolating to 100 °C. The detailed parameters of the model may vary, but qualitative conclusions can still be drawn.

To begin, the resistivity of nanotubes is only slightly lower than that of bulk copper. This means that nanotube ropes must be densely packed and made of all metallic nanotubes for the material to be competitive with bulk copper for large cross sectional area interconnects. On the other hand, for sub-100-nm cross-sectional-area interconnects, the performance of copper degrades significantly, so that nanotube ropes may be advantageous even if they are not densely packed or consist of some fraction of semiconducting nanotubes. An additional note is that the exact value of the nanotube resistivity (and its variation with diameter and temperature) is not yet established, nor are the parameters in the Cu interconnect plot. So, care needs to be taken when comparing the performance predictions of both materials in regimes (such as sub-10-nm line-width traces) where the knowledge is primarily theoretical and not experimental. Regardless of these uncertainties the primary conclusion is that the resistivity of SWNTs is lower than bulk copper, and that surface scattering (which plagues copper at narrow line widths) is not an issue for SWNTs. These conclusions have motivated more detailed studies comparing Cu to SWNTs in various applications, discussed and summarized below.

13.2. Frequency-Dependent Impedance of an Individual SWNT

The above discussions in this paper have dealt with the transmission line model for a single nanotube or two nanotubes. As a function of frequency, how important is the transmission line model? This depends on the frequency range of interest. In order to illustrate this point, in Figure 19, we plot our calculations of the real nanotube impedance vs. frequency of an individual SWNT for a realistic length of 100 μm and resistance per length of $\frac{1\,k\Omega}{\mu m}$. These were numerically calculated using the circuit model show in Figure 10, and include the distributed (diffusive) resistance *and* the quantum contact resistance.

The qualitative origins of the impedance versus frequency in Figure 19 are easy to understand. In the low-frequency limit, the impedance becomes the dc resistance. As the frequency increases, one sees an "RC"- type rolloff. At much higher frequencies, the system looks like a transmission line, and the impedance becomes the characteristic impedance of the transmission line. The frequency at which this occurs is given by the inverse of the effective "L/R" time constant, which is the resistance per unit length divided by the inductance per unit length.

The characteristic impedance of any transmission line is given by the square root of the inductance divided by the capacitance per unit length. In this case, that works out to be (using Equations (10) and (17)):

$$Z_C \approx \frac{h}{2e^2} = 12\,k\Omega \tag{58}$$

If one includes the electrostatic capacitance also, the result is different by a factor of order unity.[57–60] This comes back to the initial problem of impedance mismatch. In fact, since the nanotube transmission line impedance is of order the resistance quantum, and typical nanotube (and other nanoscale) devices have impedances of order the resistance quantum, this in effect *solves* the impedance mismatch

problem, if all nanodevices are connected to each other through nanotube transmission lines. This motivates the vision of *integrated nanosystems*.[2]

13.3. Inductance at GHz Frequencies is Unimportant

As discussed above, the qualitative frequency dependent impedance at frequencies below the L/R time is approximately that of an RC circuit. The inductance is numerically not important, and therefore the transmission line effects are not significant. What is this frequency numerically? Since we know the resistance per unit length and inductance per unit length, we can use the following expression to determine the frequency at which inductive effects (and hence transmission line effects) become significant:

$$i\omega L > R \tag{59}$$

Numerically, this corresponds to the following:

$$f > \frac{R}{2\pi L} \approx 200\,GHz \tag{60}$$

Therefore, for GHz frequencies the kinetic inductance and transmission line effects are not significant; it is only in the THz range that these effects are important. We also note that there is no inductive crosstalk due to the kinetic inductance. Thus, for applications in interconnects the primary focus is the dc resistance and the capacitance.

13.4. Ideal Bundles of all Metallic SWNTs of Various Geometries

The use of an individual SWNT would be too resistive for coupling to any envisioned CMOS active device. Therefore, it is clear the bundles of nanotubes should be used. We begin with a discussion of an ideal bundle of all metallic nanotubes with location that can be controlled at will. First, consider the R, L, C of a bundle of unspecified geometry. What general conclusions can be made regardless of the detailed geometry of the bundle? The resistance of a bundle goes down as the number of tubes in the bundle increases. The capacitance is only weakly dependent on number of tubes in the bundle, since it depends primarily on the electric field distribution outside of the bundle. Thus, the RC time immediately is seen to decrease strongly by adding more nanotubes to the bundle. The kinetic inductance (already unimportant at GHz frequencies) also decreases linearly with the number of tubes, and so is still insignificant. Thus, using nanotube bundles provides a significant decrease in RC time delays regardless of the detailed geometry of the bundle.

Naeemi and Meindl have performed a detailed analysis of the performance of nanotube bundles of the two main possible geometries: square arrays and monolayer arrays of SWNTs, and compared to copper interconnects, for various technology nodes and interconnect lengths. In Figure 20 (from Naeemi),[74] the RC delay versus interconnect length is plotted for a 27-nm Cu trace, and two different nanotube bundle geometries: a square array (250 metallic SWNTs) and a multilayer array (20 metallic SWNTs). For long lengths, the bundles are faster because of the lower resistance. For short lengths, the thin multilayer geometry is faster because of lower capacitance. (The difference between the square array and multilayer array matters.)

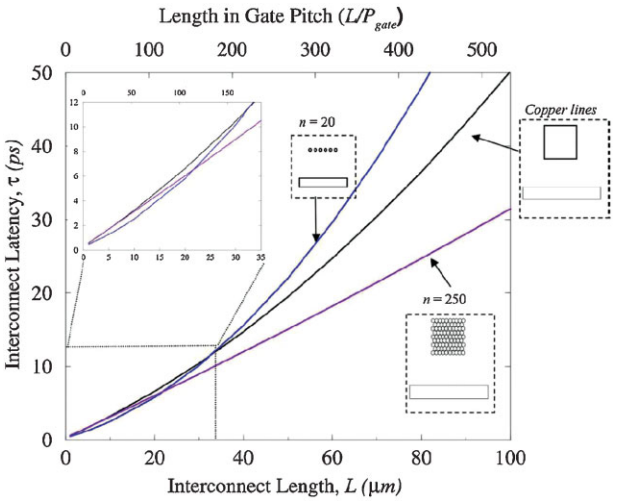

Figure 20. RC delay versus interconnect length for a 27-nm Cu trace, and two different nanotube bundle geometries: a square array (250 metallic SWNTs) and a multilayer array (20 metallic SWNTs). For long lengths, the bundles are faster because of the lower resistance. For short lengths, the thin multilayer geometry is faster because of lower capacitance. Reproduced with permission from Reference [74]. Copyright 2007, IEEE Transactions on Electron Devices.

Additional analysis of the local, semiglobal, and global interconnects has been performed by the Meindl group for various nanotube bundle geometries.[45,70,71,74–83] They find that for local interconnects, monolayers or multilayer interconnects can reduce the RC delay by up to 20%. For semiglobal interconnects, nanotubes bundles can achieve higher conductivity, which can translate into lower delay or lower power dissipation. The latter is potentially important since a significant fraction of total power dissipation in modern ICs occurs in the interconnects. For global interconnects, the cross sectional dimensions are typically large. Therefore, the advantage of nanotubes over copper becomes less significant, since one must attain a bulk conductivity of copper by using dense ropes of SWNTs.

These types of numerical simulations provide valuable design guidance for the improvement that can be expected for SWNT interconnects. However, unfortunately the technology does not yet exist to fabricated these ideal bundles to test these projections, although progress along the lines is occurring and eventually prototype tests will be possible.[84]

As a final note, the RC time itself is not the only figure of merit to compare nantoubes to copper. For example, Saraswat at Stanford has provided an analysis and comparison of the RC time/bandwidth per power dissipated as another figure of merit,[85–89] and developed comparisons to optical interconnects, as well. In general, lower RC delays are just one of a comlex set of metrics that must be used when considering any potential material to replace Cu as an interconnect.

NANO MICRO small

13.5. Non-ideal Bundles

While an ideal interconnect would consist of all metallic nanotubes in a bundle of user defined geometry, in reality SWNTs are synthesized as a mixture of semiconducting and metallic SWNTs. In fact, statistically the fraction of nanotubes is 1/3 metallic and 2/3 semiconducting. Various groups have attempted to model these non-idealities and their impact on the electric performance of non-ideal bundles. Massoud at Rice focused on mixtures of metallic and semiconducting nanotubes, and develop methods to carefully predict the magnetic inductance of these.[90–104] Banjeree at UCSB did simulations of SWNTs and MWNTs, including thermal effects.[105–111] Wang at Purdue analyzed mixed bundles of SWNTs and MWNTs.[112] This work is significant and important for present day synthesis technology, which is incapable of producing all metallic nanotube bundles of desired and arbitrary geometry. One hopes that someday the technology will be developed to do this, which will allow the projected performance of ideal bundles to be achieved.

13.6. Multi-Walled Nanotubes

For via interconnects and DRAM, the use of multi-walled nanotubes is a possibility since they can be grown inside of holes with high aspect ratios. Indeed, several groups (including NASA,[113–118] Fujitsu,[119–126] and Infeneon[127–134]) have focused on improving synthesis techniques for this purpose. The Wong group at Stanford recently demonstrated a 1 GHz circuit with CMOS transistors connected in part with MWNT interconnects.[135] Unfortunately the resistance achieved to date has not been below than that achievable with copper, and the theoretical reasons for this have not yet been completely determined. It is in principle possible, and if so then MWNTs may outperform Cu for long interconnects.[70] Thus, it is unknown at this stage whether it is possible to fabricate MWNTs with resistivity lower than copper, whereas for SWNTs it is well known.

14. Nanotube Antennas

14.1. Introduction

One final area of potential application is in the use of nanotubes as antennas. So far in the RF and microwave, no experiments have been reported on this topic.

Optical ''antennas'' were recently demonstrated.[136] However, there have been some theoretical developments. The essential idea is captured schematically in Figure 21 below.[137] This idea could be useful for any application in which wireless contact to a nanoscale device is required, for example, nanoscale sensors.

14.2. Nanotube Dipole

One of the most fundamental parameters of any antenna is the current distribution on the antenna. This determines the radiation pattern, the radiation resistance and reactance, and many other properties of interest. Modern work on antenna theory is typically numerical because of the lack of analytical solutions. In contrast, early work on antenna theory (including some pioneers such as Hallen and Schelkunoff) focused on deriving analytical expressions for the current distribution on an antenna.[138–142]

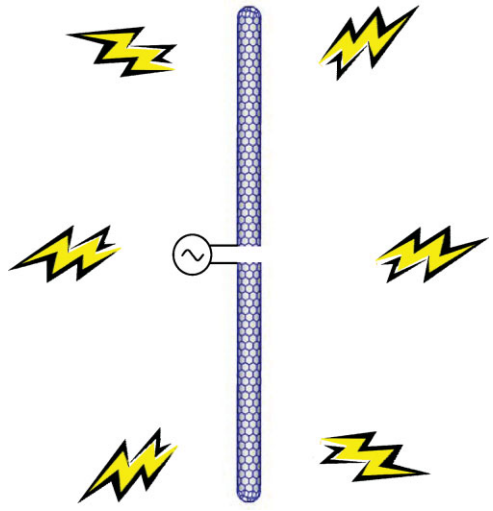

Figure 21. Concept of nanotube antenna. Because nanotubes of lengths up to several cm can be grown, we have asked whether and how they may function as antennas. Reproduced with permission from Reference [137]. Copyright 2005, Proceedings of the 9th International Conference on Electromagnetic in Advanced Applications.

In their work, the only geometry to which an analytical solution is available (to our knowledge) is the simple dipole antenna. Analytical expressions are available as series expansions in the parameter $\frac{d}{l}$, where d is the diameter and l the length. Virtually all of modern antenna theory takes as its canonical example the characteristics of a dipole antenna in the limit $\frac{d}{l}$ goes to zero.

Now, with the advent of cm-long carbon nanotubes, it is possible to fabricate conducting wires with unprecedented aspect ratios of order 10^7. This has led us to propose a nanotube antenna, shown in Figure 21. At first sight, it would seem that this new system would be the closest physical realization to a dipole antenna (in the sense that $\frac{d}{l}$ is small) mankind has ever manufactured. However, this is not the case, as we elaborate on below.

14.3. Nanotube Versus Classical Antenna

In original theoretical work on dipole antennas, it was assumed that the dipole radius was larger than the skin depth, and that the resistive losses were low enough to be neglected in determining the current distribution on the antenna. Both of these assumptions break down for nanotube antennas. Therefore, the original theory and hence the only analytical theory breaks down in the limit $\frac{d}{l}$ becomes sufficiently small.

In a one-dimensional conductor such as a nanotube, the concept of skin-depth is almost meaningless, since the electrons are only free to move along the length of the wire, and not in the transverse direction. Therefore the current distribution is effectively one-dimensional. In addition to the

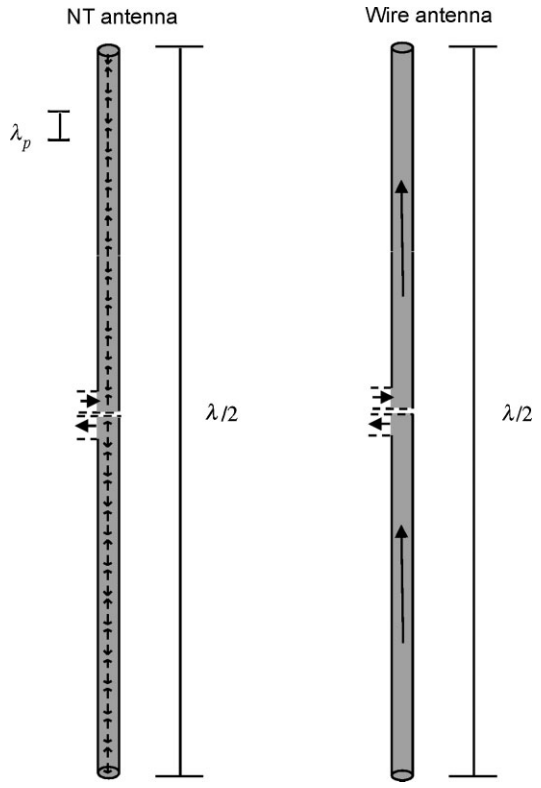

Figure 22. Current distribution on a nanotube antenna versus classical wire antenna. λ is the free space wavelength, and λ_p is the wavelength of the current distribution on a nanotube. Because of the large kinetic inductance, the wave velocity is 100 times smaller (and thus the wavelength for the current distribution is 100 times smaller) than an electromagnetic wave for a given (temporal) frequency. Reproduced with permission from Reference [143]. Copyright 1999, IEEE Transactions on Microwave Theory and Techniques.

electron transport occurring in only one dimension, we also have two more important effects: large resistance, and large inductance.

These effects give rise to very different behavior for a nanotube antenna, as compared to a classical antenna. The main difference is that the current distribution is periodic with a wavelength about 100 times smaller than the free space wavelength for a given temporal frequency. The physics behind this phenomenon is straightforward to explain: The wavelength of the current distribution (for a given frequency) depends on the wave velocity of the mode. If the wave velocity is the speed of light, then the wavelength of the current distribution is of order the wavelength of the electromagnetic wave in free space. On the other hand, in a nanotube the wave velocity is typically about 100 times smaller than the speed of light. This is because the wave velocity (in circuit terms) is given by the inverse of the square root of the capacitance per unit length times the inductance per unit length. As we have discussed above, the kinetic inductance per unit length in nanotubes is about 10 000 times larger than the magnetic inductance per unit length, hence the wave velocity is 100 times smaller than the speed of light.

The comparison of the current distribution on a nanotube dipole antenna to a classical dipole antenna is shown in Figure 22 below.[143] It is clear that the current distributions are dramatically different. Our work has been further developed numerically by Hanson.[7]

14.4. Efficiency

Our calculations show that the efficiency of a classical nanotube dipole antenna is of the order −90 dB, due to resistive losses.[8] However, we have proposed that possibly other geometries (to be determined) could and should be investigated that take advantage of the unique materials and electronic properties of carbon nanotubes.

14.5. Scattering Antenna

Recent work in the optical has interpreted scattering experiments of vertically aligned multi-walled carbon nanotubes as an antenna effect. While optical antennas do not act to couple radiation to circuit in the same way as RF antennas, they can have frequency-dependent resonant scattering effects that are dependent on the length of the nanotube, and hence be considered antennas as well in this sense. Such a scattering experiment is indicated schematically in Figure 23 below.

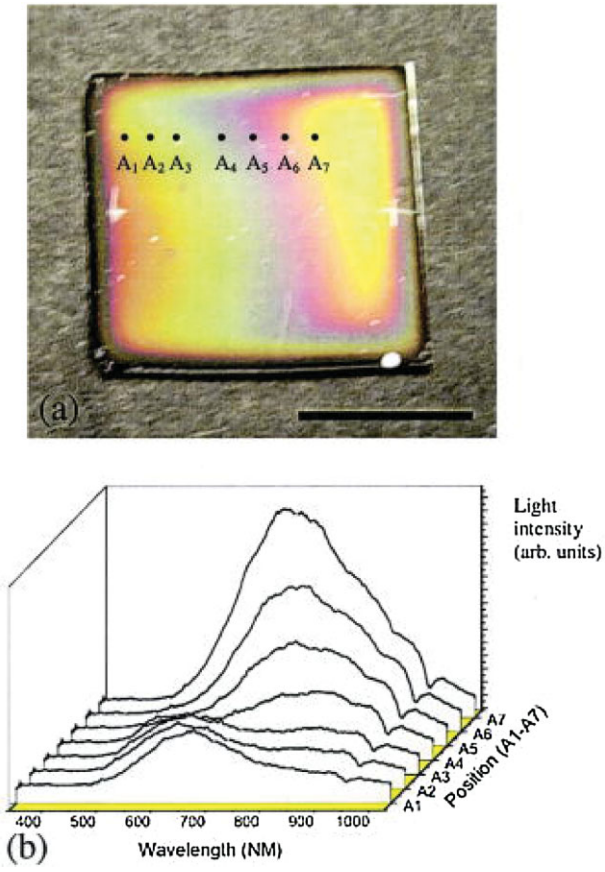

Figure 23. Optical nanotube scattering antennas. The wafer consists of a "forest" of nanotubes, whose length depends on the position along the wafer. Experiments show that the scattered light peaks at a wavelength that also depends on the position along the wafer, which is attributed to a collective optical antenna effect due to the finite length of the nanotubes. Reproduced with permission from Reference [136]. Copyright 2004, Applied Physics Letters.

NANO MICRO small

14.6. Next Step: Metamaterials?

The development of metamaterials is based largely on the artificial engineering of electromagnetic structures with periodicity less than the electromagnetic wavelength, but larger than atomic size.[144–154] We speculate that a next possible step for nanotubes as antennas is in the application of such metamaterials. This would require further development along the theoretical lines discussed in this manuscript to understand the scattering properties of such structures. In addition, nanofabrication techniques would have to continue to advance.

We have shown in the first section of this paper that the synthesis of nanotubes has been developing rapidly, and currently the longest SWNTs synthesized are over 1 cm long. The next step in synthesis challenges will be to develop densely spaced SWNTs that are well aligned. In Figure 24, we show an SEM image of an array synthesized in our lab. Such arrays of horizontally grown SWNTs have a pitch of typically 10–100 nm, which leaves much room for tailoring properties. A current effort is underway to reduce such a pitch, and to be able to control and engineer it at will.[155–157] At the moment, this is still an elusive goal, but not insurmountable. A second technique has recently been developed to synthesize vertically oriented, mm-long SWNTs over macroscopic areas.[158] Thus, the advances in nanoscale fabrication are rapid and will most likely continue to improve our ability to rationally control and engineer large-scale structures with nanometer precision.

15. Summary and Outlook

A more general theory of nanotube ''antennas'' that applies even in the optical frequency range to scattering experiments has been developed.[62–67,136] However the full application and power of this theory is still very much under development. Thus the application of the concept of antenna is really not limited just to the RF frequency range. However, much theoretical and experimental work remains to be done to truly understand and utilize the concepts in engineering applications.

In summary, we have presented the most up-to-date understanding of the electromagnetic properties of carbon nanotubes as interconnects and antennas. In the area of interconnects, circuit models have already been developed theoretically by several techniques, which agree when the realms of application overlap. In the area of antennas, the topic is too new for there to be many specific predictions of antenna properties. Where there have been predictions (which is only for a dipole), differing approaches also give similar predictions. However, for arbitrary antenna geometries at the moment little is known, other than the requirement to solve Maxwell's equations in order to understand their properties. Thus, there remains much left to do to understand nanoantennas from a theoretical point of view. Finally, the experimental results in this field are few and far between. This is primarily because of the difficulty in fabrication and measurement. Fabrication advances are occurring rapidly, and measurement techniques need to be developed and applied to keep pace with the rapid fabrication advances. Only then will a full understanding of an increasingly technologically relevant field of inquiry, that of nano-electromagnetics be achieved.

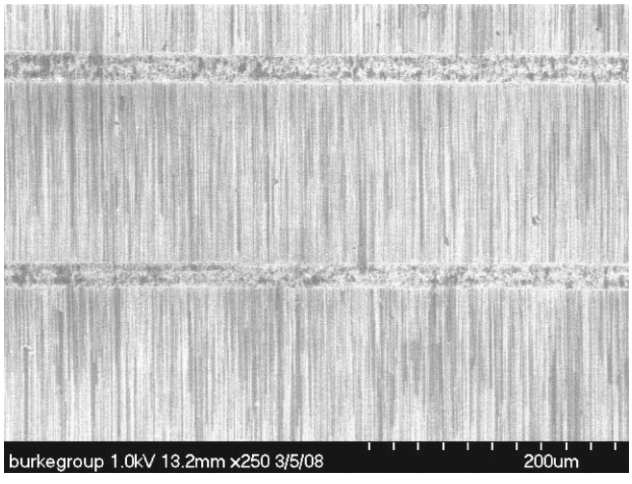

Figure 24. Aligned array of SWNTs synthesized on a single-crystal quartz or sapphire can be very dense (with pitch less then 50 nm), and very aligned, on a wafer scale. Reproduced with permission from Reference [159]. Copyright 2008, Nano Research.

Acknowledgements

We acknowledge fruitful collaborations with our students and postdocs Zhen Yu, Shengdong Li, and Weiwei Zhou. This work was supported by the ARO, ONR, NSF, and DARPA.

Keywords:

carbon nanotubes · electromagnetic materials · nanoelectromagnetism

[1] P. Burke, *Nanotubes and Nanowires*, World Scientific, **2007**.
[2] P. J. Burke, *Solid State Electron.* **2004**, *40*, 10.
[3] R. D. Grober, R. J. Schoelkopf, D. E. Prober, *Appl. Phys. Lett.* **1997**, *70*, 11.
[4] K. B. Crozier, A. Sundaramurthy, G. S. Kino, C. F. Quate, *J. Appl. Phys.* **2003**, *94*, 7.
[5] D. K. Ferry, S. M. Goodnick, *Transport in Nanostructures*, Cambridge University Press, Cambridge, UK **1997**.
[6] J. Gabelli, G. Feve, J. M. Berroir, B. Placais, A. Cavanna, B. Etienne, Y. Jin, D. C. Glattli, *Science* **2006**, *313*, 5786.
[7] G. W. Hanson, *IEEE Trans. Antennas Propag.* **2005**, *53*, 11.
[8] P. Burke, Z. Yu, S. Li, *cond-mat/0408418* **2004**.
[9] M. S. Dresselhaus, G. Dresselhaus, P. Avouris, *Carbon Nanotubes: Synthesis, Structure, Properties, and Applications*, Springer, Berlin **2001**.
[10] M. S. Dresselhaus, G. Dresselhaus, P. C. Eklund, *Science of Fullerenes and Carbon Nanotubes*, Academic Press, San Diego **1996**.
[11] P. J. F. Harris, *Carbon Nanotubes and Related Structures: New Materials for the Twenty-First Century*, Cambridge University Press, Cambridge, UK **1999**.
[12] M. Meyyappan, *Carbon Nanotubes: Science and Applications*, CRC Press, Boca Raton, FL **2005**.
[13] S. Reich, C. Thomsen, J. Maultzsch, *Carbon Nanotubes: Basic Concepts and Physical Properties*, Wiley-VCH, Weinheim **2004**.

[14] K. Tanaka, T. Yamabe, K. I. Fukui, *The Science and Technology of Carbon Nanotubes*, 1st ed., Elsevier, Amsterdam **1999**.
[15] R. Saito, G. Dresselhaus, M. S. Dresselhaus, *Physical Properties of Carbon Nanotubes*, Imperial College Press, London **1998**.
[16] S. Li, Z. Yu, C. Rutherglen, P. J. Burke, *Nano Lett.* **2004**, *4*, 10.
[17] S. Datta, *Electronic Transport in Mesoscopic Systems*, Cambridge University Press, Cambridge **1995**.
[18] H. Grabert, M. H. Devoret, North Atlantic Treaty Organization. Scientific Affairs Division, *Single Charge Tunneling: Coulomb Blockade Phenomena in Nanostructures*, Plenum Press, New York **1992**.
[19] J. J. Plombon, K. P. O'Brien, F. Gstrein, V. M. Dubin, Y. Jiao, *Appl. Phys. Lett.* **2007**, *90*, 6.
[20] A. Tselev, M. Woodson, C. Qian, J. Liu, *Nano Lett.* **2008**, *8*, 1.
[21] S. C. Jun, J. H. Choi, S. N. Cha, C. W. Baik, S. Lee, H. J. Kim, J. Hone, J. M. Kim, *Nanotechnology* **2007**, *18*, 25.
[22] P. Rice, T. M. Wallis, S. E. Russek, P. Kabos, *Nano Lett.* **2007**, *7*, 4.
[23] J. Chaste, L. Lechner, P. Morfin, G. Feve, T. Kontos, J. M. Berroir, D. C. Glattli, H. Happy, P. Hakonen, B. Placais, *Nano Lett.* **2008**, *8*, 2.
[24] S. Li, Z. Yu, S. F. Yen, W. C. Tang, P. J. Burke, *Nano Lett.* **2004**, *4*, 4.
[25] Z. Yu, P. J. Burke, *Nano Lett.* **2005**, *5*, 7.
[26] D. Wang, Z. Yu, S. McKernan, P. J. Burke, *IEEE Trans. Nanotechnol.* **2007**, *6*, 4.
[27] C. Kocabas, H. S. Kim, T. Banks, J. A. Rogers, A. A. Pesetski, J. E. Baumgardner, S. V. Krishnaswamy, H. Zhang, *Proc. Nat. Acad. Sci. U. S. A.* **2008**, *105*, 5.
[28] C. Rutherglen, D. Jain, P. Burke, *Appl. Phys. Lett.* **2008**, *93*, 8.
[29] A. Le Louarn, F. Kapche, J. M. Bethoux, H. Happy, G. Dambrine, V. Derycke, P. Chenevier, N. Izard, M. F. Goffman, J. P. Bourgoin, V. Derycke, P. Chenevier, N. Izard, M. F. Goffman, J. P. Bourgoin, *Appl. Phys. Lett.* **2007**, *90*, 23.
[30] P. L. McEuen, M. S. Fuhrer, H. K. Park, *IEEE Trans. Nanotechnol.* **2002**, *1*, 1.
[31] S. Datta, *Quantum Transport: Atom to Transistor*, Cambridge, **2005**.
[32] A. Javey, J. Guo, Q. Wang, M. Lundstrom, H. J. Dai, *Nature* **2003**, *424*, 6949.
[33] A. Javey, J. Guo, M. Paulsson, Q. Wang, D. Mann, M. Lundstrom, H. J. Dai, *Phys. Rev. Lett.* **2004**, *92*, 10.
[34] A. Javey, P. F. Qi, Q. Wang, H. J. Dai, *Proc. Nat. Acad. Sci. U. S. A.* **2004**, *101*, 37.
[35] Y. Fan, B. R. Goldsmith, P. G. Collins, *Nat. Mater.* **2005**, 4.
[36] J. Y. Park, S. Rosenblatt, Y. Yaish, V. Sazonova, H. Ustunel, S. Braig, T. A. Arias, P. W. Brouwer, P. L. McEuen, *Nano Lett.* **2004**, *4*, 3.
[37] M. S. Purewal, B. H. Hong, A. Ravi, B. Chandra, J. Hone, P. Kim, *Phys. Rev. Lett.* **2007**, *98*, 18.
[38] T. Durkop, S. A. Getty, E. Cobas, M. S. Fuhrer, *Nano Lett.* **2004**, *4*, 1.
[39] Y.-F. Chen, M. S. Fuhrer, *Phys. Rev. Lett.* **2005**, 95.
[40] B. H. Hong, J. Y. Lee, T. Beetz, Y. M. Zhu, P. Kim, K. S. Kim, *J. Am. Chem. Soc.* **2005**, *127*, 44.
[41] Z. Yao, C. L. Kane, C. Dekker, *Phys. Rev. Lett.* **2000**, *84*, 13.
[42] A. Raychowdhury, S. Mukhopadhyay, K. Roy, *IEEE Trans. Computer-Aided Design Integ. Circu. Syst.* **2004**, *23*, 10.
[43] A. Raychowdhury, K. Roy, *IEEE Trans. Computer-Aided Design of Integ. Circui. Syst. [0278–0070] Raychowdhury* **2006**, *25*, 1.
[44] A. Raychowdhury, K. Roy, *Nanotechnology, 4th IEEE Conference on*. **2004**.
[45] A. Naeemi, J. D. Meindl, *IEEE Electron Device Lett.* **2005**, *26*, 7.
[46] *International Technology Roadmap for Semiconductors*; http://public.itrs.net/ **2007**.
[47] W. Steinhogl, G. Schindler, G. Steinlesberger, M. Traving, M. Engelhardt, *J. Appl. Phys.* **2005**, *97*, 2.
[48] J. O. J. Wesstrom, *Phys. Rev. B* **1996**, *54*, 16.
[49] V. V. Ponomarenko, *Phys. Rev. B* **1996**, *54*, 15.
[50] M. Buttiker, *J. Low Temp. Phys.* **2000**, *118*, 5–6.
[51] V. A. Sablikov, B. S. Shchamkhalova, *JETP Lett.* **1997**, *66*, 1.
[52] Y. M. Blanter, F. W. J. Hekking, M. Buttiker, *Phys. Rev. Lett.* **1998**, *81*, 9.
[53] G. Cuniberti, M. Sassetti, B. Kramer, *Phys. B* **1996**, *227*, 1–4.
[54] G. Cuniberti, M. Sassetti, B. Kramer, *J. Phys. Condens. Matter* **1996**, *8*, 2.
[55] G. Cuniberti, M. Sassetti, B. Kramer, *Phys. Rev. B* **1998**, *57*, 3.
[56] V. A. Sablikov, B. S. Shchamkhalova, *J. Low Temp. Phys.* **2000**, *118*, 5–6.
[57] P. J. Burke, *IEEE Trans. Nanotechnol.* **2002**, *1*, 3.
[58] P. J. Burke, *IEEE Trans. Nanotechnol.* **2003**, *2*, 1.
[59] P. J. Burke, *IEEE Trans. Nanotechnol.* **2004**, *3*, 2.
[60] P. J. Burke, *IEEE Trans. Nanotechnol.* **2004**, *3*, 2.
[61] S. Salahuddin, M. Lundstrom, S. Datta, *IEEE Trans. Electron. Devices.* **2005**, *52*, 8.
[62] O. M. Yevtushenko, G. Y. Slepyan, S. A. Maksimenko, A. Lakhtakia, D. A. Romanov, *Phys. Rev. Lett.* **1997**, *79*, 6.
[63] G. Y. Slepyan, S. A. Maksimenko, A. Lakhtakia, O. M. Yevtushenko, A. V. Gusakov, *Phys. Rev. B* **1998**, *57*, 16.
[64] A. Lakhtakia, G. Y. Slepyan, S. A. Maksimenko, A. V. Gusakov, O. M. Yevtushenko, *Carbon* **1998**, *36*, 12.
[65] G. Y. Slepyan, S. A. Maksimenko, A. Lakhtakia, O. Yevtushenko, A. V. Gusakov, *Phys. Rev. B* **1999**, *60*, 24.
[66] G. Y. Slepyan, N. A. Krapivin, S. A. Maksimenko, A. Lakhtakia, O. M. Yevtushenko, *Aeu-Int. J. Elect. Commun.* **2001**, *55*, 4.
[67] G. Y. Slepyan, S. A. Maksimenko, A. Lakhtakia, O. M. Yevtushenko, *Synthe. Meta.* **2001**, *124*, 1.
[68] M. P. A. Fisher, L. I. Glazman, Transport in one-dimensional Luttinger liquid, In *Mesoscopic Electron Transport* (Eds.: L. L. Sohn, L. P. Kouwenhoven, G. Schèon, N. A. T. O. S. A. Division), Kluwer Academic Publishers, Dordrecht; Boston **1997**.
[69] K. V. Pham, *Eur. Phys. J. B* **2003**, *36*, 4.
[70] A. Naeemi, R. Sarvari, J. D. Meindl, *IEEE Electron Device Lett.* **2005**, *26*, 2.
[71] A. Naeemi, J. D. Meindl, *IEEE Electron Device Lett.* **2005**, *26*, 8.
[72] S. Ramo, J. R. Whinnery, T. Van Duzer, *Fields and waves in communication electronics*, 3rd edn., Wiley, New York **1994**.
[73] V. Zhirnov, D. Herr, M. Meyyappan, *J. Nanoparticle Res.* **1999**, *1*, 1.
[74] A. Naeemi, J. D. Meindl, *IEEE Trans. Electron. Devices.* **2007**, *54*, 1.
[75] A. Naeemi, J. D. Meindl, *IEEE Electron Device Lett.* **2006**, *27*, 5.
[76] A. Naeemi, R. Sarvari, J. D. Meindl, *International Interconnect Technology Conference* **2006**.
[77] A. Naeemi, G. Huang, J. D. Meindl, *Electronic Components and Technology Conference*, **2007**.
[78] A. Naeemi, J. D. Meindl, *Proceedings of the 2007 International Symposium on Physical Design* **2007**.
[79] A. Naeemi, J. D. Meindl, *IEEE Electron. Device. Lett.* **2007**, *28*, 2.
[80] A. Naeemi, J. D. Meindl, *IEEE Electron. Device. Lett.* **2007**, *28*, 5.
[81] A. Naeemi, R. Sarvari, J. D. Meindl, *Proceedings of the 44th Annual Conference on Design Automation*. **2007**.
[82] A. Naeemi, J. D. Meindl, *IEEE Trans. Electron. Devices.* **2008**, *55*, 10.
[83] A. Naeemi, J. D. Meindl, *International Interconnect Technology Conference* **2008**.
[84] C. Rutherglen, D. Jain, P. Burke, *Appl. Phys. Lett.* **2008**, 93.
[85] H. Cho, K. Koo, P. Kapur, K. Saraswat, *IEEE International Interconnect Technology Conference* **2007**.
[86] H. Cho, K. Koo, P. Kapur, K. Saraswat, *Proceedings of the 2007 International Workshop on System Level Interconnect Predication* **2007**.
[87] H. Cho, K. H. Koo, P. Kapur, K. C. Saraswat, *IEEE Electron. Device. Lett.* **2008**, *29*, 1.
[88] K. H. Koo, H. Cho, P. Kapur, K. C. Saraswat, *IEEE Trans. Electron. Devices.* **2007**, *54*, 12.
[89] K. Saraswat, H. Cho, P. Kapur, K. Koo, *IEEE International Symposium on Circuits and Systems* **2008**.

[90] Y. Massoud, A. Nieuwoudt, *6th IEEE Conference on Nanotechnology*, **2006**, 1.
[91] Y. Massoud, A. Nieuwoudt, *1st International Conference on Nano-Networks and Workshops*, **2006**.
[92] Y. Massoud, A. Nieuwoudt, *6th IEEE Conference on Nanotechnology*, **2006**, 1.
[93] Y. Massoud, A. Nieuwoudt, *ACM J. Emerg. Tech. Comput. Syst. (JETC)* **2006**, *2*, 3.
[94] A. Nieuwoudt, Y. Massoud, *IEEE Trans. Nanotechnol.* **2006**, *5*, 6.
[95] A. Nieuwoudt, Y. Massoud, *IEEE Trans. Electron. Devices.* **2006**, *53*, 10.
[96] S. Eachempati, A. Nieuwoudt, A. Gayasen, N. Vijaykrishnan, Y. Massoud, *Proceedings of the Conference on Design, Automation and Test in Europe* **2007**.
[97] A. Nieuwoudt, Y. Massoud, *Nanotechnology, IEEE-NANO2007.7th IEEE Conference on* **2007**.
[98] A. Nieuwoudt, Y. Massoud, *IEEE Electron. Device. Lett.* **2007**, *28*, 4.
[99] A. Nieuwoudt, Y. Massoud, *IEEE Trans. Electron. Devices.* **2007**, *54*, 3.
[100] Y. Massoud, A. Nieuwoudt, *IEEE International Symposium on Circuits and Systems* **2008**.
[101] A. Nieuwoudt, Y. Massoud, *IEEE Trans. Electron. Devices.* **2008**, *55*, 8.
[102] A. Nieuwoudt, Y. Massoud, *9th International Symposium on Quality Electronic Design*, **2008**.
[103] A. Nieuwoudt, Y. Massoud, *IEEE Trans. Electron. Devices.* **2008**, *55*, 1.
[104] T. Ragheb, A. Nieuwoudt, Y. Massoud, *51st Midwest Symposium on Circuits and Systems*, **2008**.
[105] N. Srivastava, K. Banerjee, *Jom* **2004**, *56*, 10.
[106] N. Srivastava, K. Banerjee, *Proc. VMIC* **2004**.
[107] N. Srivastava, K. Banerjee, *IEEE/ACM International Conference on Computer-Aided Design*, **2005**.
[108] N. Srivastava, R. Joshi, K. Banerjee, *IEEE International Electron Devices Meeting*, **2005**.
[109] K. Banerjee, N. Srivastava, *Proceedings of the 43rd Annual Conference on Design Automation* **2006**.
[110] H. Li, N. Srivastava, J. Mao, W. Yin, K. Banerjee, *IEEE International Electron Devices Meeting*, **2007**.
[111] H. Li, W. Y. Yin, K. Banerjee, J. F. Mao, *IEEE Trans. Electron. Devices.* **2008**, *55*, 6.
[112] S. Haruehanroengra, W. Wang, *IEEE Electron Device Lett.* **2007**, *28*, 8.
[113] J. Li, Q. Ye, A. Cassell, H. T. Ng, R. Stevens, J. Han, M. Meyyappan, *Appl. Phys. Lett.* **2003**, *82*, 15.
[114] Q. Ngo, D. Petranovic, S. Krishnan, A. Cassell, Q. Ye, J. Li, M. Meyyappan, C. Yang, *IEEE Trans. Nanotechnol.* **2004**, *3*, 2.
[115] Y. Ominami, Q. Ngo, A. J. Austin, H. Yoong, C. Y. Yang, A. M. Cassell, B. A. Cruden, J. Li, M. Meyyappan, *Appl. Phys. Lett.* **2005**, *87*, 23.
[116] Q. Ngo, A. M. Cassell, A. J. Austin, J. Li, S. Krishnan, M. Meyyappan, C. Y. Yang, *IEEE Electron Device Lett.* **2006**, *27*, 4.
[117] Q. Ngo, A. M. Cassell, V. Radmilovic, J. Li, S. Krishnan, M. Meyyappan, C. Y. Yang, *Carbon* **2007**, *45*, 2.
[118] Q. Ngo, T. Yamada, M. Suzuki, Y. Ominami, A. M. Cassell, J. Li, M. Meyyappan, C. Y. Yang, *IEEE Trans. Nanotechnol.* **2007**, *6*, 6.
[119] M. Nihei, M. Horibe, A. Kawabata, Y. Awano, *Jpn. J. Appl. Phys. Part 1-Regular Papers Short Notes & Review Papers* **2004**, *43*, 4B.
[120] M. Nihei, M. Horibe, A. Kawabata, Y. Awano, F. Ltd, J. Atsugi, *Proceedings of the IEEE2004 International Interconnect Technology Conference* **2004**.
[121] M. Nihei, A. Kawabata, D. Kondo, M. Horibe, S. Sato, Y. Awano, *Jpn. J. Appl. Phys. Part 1-Regular Papers Short Notes & Review Papers* **2005**, *44*, 4.
[122] M. Nihei, D. Kondo, A. Kawabata, S. Sato, H. Shioya, M. Sakaue, T. Iwai, M. Ohfuti, Y. Awano, *Proceedings of the IEEE International Interconnect Technology Conference* **2005**.
[123] Y. Awano, S. Sato, D. Kondo, M. Ohfuti, A. Kawabata, M. Nihei, N. Yokoyama, *Phys. Stat. Solidi A-Appl. Mater. Sci.* **2006**, *203*, 14.
[124] S. Sato, M. Nihei, A. Mimura, A. Kawabata, D. Kondo, H. Shioya, T. Iwai, M. Mishima, M. Ohfuti, Y. Awano, *International Interconnect Technology Conference* **2006**.
[125] M. Nihei, T. Hyakushima, S. Sato, T. Nozue, M. Norimatsu, M. Mishima, T. Murakami, D. Kondo, A. Kawabata, M. Ohfuti, *IEEE International Interconnect Technology Conference* **2007**.
[126] D. Yokoyama, T. Iwasaki, T. Yoshida, H. Kawarada, S. Sato, T. Hyakushima, M. Nihei, Y. Awano, *Appl. Phys. Lett.* **2007**, *91*, 26.
[127] F. Kreupl, A. P. Graham, G. S. Duesberg, W. Steinhogl, M. Liebau, E. Unger, W. Honlein, *Microelect. Eng.* **2002**, *64*, 1–4.
[128] G. S. Duesberg, A. P. Graham, M. Liebau, R. Seidel, E. Unger, F. Kreupl, W. Hoenlein, *Nano Lett.* **2003**, *3*, 2.
[129] W. Hoenlein, F. Kreupl, G. S. Duesberg, A. P. Graham, M. Liebau, R. Seidel, E. Unger, *Mater. Sci. Eng. C-Biomimetic Supramole. Syst.* **2003**, *23*, 6–8.
[130] G. S. Duesberg, A. R. Graham, F. Kreupl, M. Liebau, R. Seidel, E. Unger, W. Hoenlein, *Diamond Relat. Materi.* **2004**, *13*, 2.
[131] A. P. Graham, G. S. Duesberg, W. Hoenlein, F. Kreupl, M. Liebau, R. Martin, B. Rajasekharan, W. Pamler, R. Seidel, W. Steinhoegl, E. Unger, *Appl. Phys. A-Materi. Sci. & Process.* **2005**, *80*, 6.
[132] F. Kreupl, A. P. Graham, M. Liebau, G. S. Duesberg, R. Seidel, E. Unger, *Electron Devices Meeting, IEDM Technical Digest. IEEE International* **2004**.
[133] A. P. Graham, G. S. Duesberg, R. V. Seidel, M. Liebau, E. Unger, W. Pamler, F. Kreupl, W. Hoenlein, *Small* **2005**, *1*, 4.
[134] W. Hoenlein, G. S. Duesberg, A. P. Graham, F. Kreupl, M. Liebau, W. Pamler, R. Seidel, E. Unger, *Microelectron. Eng.* **2006**, *83*, 4–9.
[135] G. F. Close, S. Yasuda, B. Paul, S. Fujita, H. S. P. Wong, *Nano Lett.* **2008**, *8*, 2.
[136] Y. Wang, K. Kempa, B. Kimball, J. B. Carlson, G. Benham, W. Z. Li, T. Kempa, J. Rybczynski, A. Herczynski, Z. F. Ren, *Appl. Phys. Lett.* **2004**, *85*, 13.
[137] P. J. Burke, C. Rutherglen, Z. Yu, *Proceedings of the 9th International Conference on Electromagnetics in Advanced Applications* **2005**.
[138] E. G. Hallâen, *Theoretical Investigations into the Transmitting and Receiving Qualities of Antennâae*, Almqvist and Wiksells boktryckeri-a.-b, Uppsala **1938**.
[139] S. A. Schelkunoff, *Electromagnetic Waves*, D. Van Nostrand Company, inc, New York **1943**.
[140] S. A. Schelkunoff, *Advanced Antenna Theory*, Wiley, New York **1952**.
[141] S. A. Schelkunoff, *Antennas; Theory and Practice*, Wiley, New York **1952**.
[142] S. A. Schelkunoff, *Applied Mathematics for Engineers and Scientists*, 2d ed., Van Nostrand, Princeton, N.J. **1965**.
[143] P. J. Burke, S. Li, Z. Yu, *e-print cond-mat/0408418* **2004**.
[144] J. B. Pendry, A. J. Holden, D. J. Robbins, W. J. Stewart, *IEEE Trans. Microwave Theory Tech.* **1999**, *47*, 11.
[145] V. G. Veselago, *Soviet Physics Uspekhi-Ussr* **1968**, *10*, 4.
[146] J. B. Pendry, *Phys. Rev. Lett.* **2000**, *85*, 18.
[147] D. R. Smith, J. B. Pendry, M. C. K. Wiltshire, *Science* **2004**, *305*, 5685.
[148] R. A. Shelby, D. R. Smith, S. Schultz, *Science* **2001**, *292*, 5514.
[149] R. A. Shelby, D. R. Smith, S. C. Nemat-Nasser, S. Schultz, *Appl. Phys. Lett.* **2001**, *78*, 4.
[150] T. J. Yen, W. J. Padilla, N. Fang, D. C. Vier, D. R. Smith, J. B. Pendry, D. N. Basov, X. Zhang, *Science* **2004**, *303*, 5663.
[151] S. Linden, C. Enkrich, M. Wegener, J. F. Zhou, T. Koschny, C. M. Soukoulis, *Science* **2004**, *306*, 5700.
[152] S. Zhang, W. J. Fan, N. C. Panoiu, K. J. Malloy, R. M. Osgood, S. R. J. Brueck, *Phys. Rev. Lett.* **2005**, *95*, 13.
[153] H. O. Moser, B. D. F. Casse, O. Wilhelmi, B. T. Saw, *Phys. Rev. Lett.* **2005**, *94*, 6.

[154] N. Katsarakis, G. Konstantinidis, A. Kostopoulos, R. S. Penciu, T. F. Gundogdu, M. Kafesaki, E. N. Economou, T. Koschny, C. M. Soukoulis, *Opt. Lett.* **2005**, *30*, 11.
[155] A. Ismach, L. Segev, E. Wachtel, E. Joselevich, *Angew. Chem.* **2004**, *116*, 45.
[156] S. Han, X. L. Liu, C. W. Zhou, *J. Am. Chem. Soc.* **2005**, *127*, 15.
[157] C. Kocabas, S. H. Hur, A. Gaur, M. A. Meitl, M. Shim, J. A. Rogers, *Small* **2005**, *1*, 11.
[158] K. Hata, D. N. Futaba, K. Mizuno, T. Namai, M. Yumura, S. Iijima, *Science* **2004**, *306*, 5700.

Received: April 14, 2008
Revised: January 9, 2009